

RANDOMIZED  
QUASI-MONTE CARLO  
SIMUALTIONS FOR BASKET  
OPTION PRICING WHERE  
UNDERLYING ASSETS FOLLOW  
A TIME-CHANGED MEIXNER  
LÉVY PROCESS

GUSTAV SÄFWENBERG

Master's thesis  
2016:E32



LUND UNIVERSITY

Faculty of Engineering  
Centre for Mathematical Sciences  
Mathematical Statistics

## Abstract

Using derivative securities can help investors increase their expected returns as well as minimize their exposure to risk. For a risk-averse investor, options can offer both insurance and leverage and for a more risk-loving investor they can be used as speculation. Basket option is a kind of option whose payoff depends on an arbitrary portfolio of assets. The basket is made out of a weighted sum of assets. Pricing these kinds of options require multivariate asset pricing techniques which still remains a challenge. We aim to price basket options by using different Monte Carlo methods and compare their performance. We will test both quasi-Monte Carlo methods as well as randomized quasi-Monte Carlo methods in order to try to speed up the convergence rate. We will assume a Lévy market model with stochastic volatility through an integrated CIR-process as a stochastic time change. More specifically we are going to model the data using the Meixner distribution. In order to calibrate the model parameters we use S&P 500 index vanilla options and the fast Fourier transform (FFT).

*Keywords:* Basket options, Randomized quasi-Monte Carlo, Time-changed Lévy Processes, Meixner distribution, Fast Fourier Transform

# Contents

|          |                                                                         |           |
|----------|-------------------------------------------------------------------------|-----------|
| <b>1</b> | <b>Introduction</b>                                                     | <b>4</b>  |
| <b>2</b> | <b>Theory</b>                                                           | <b>6</b>  |
| 2.1      | Pricing of Derivatives . . . . .                                        | 6         |
| 2.1.1    | Pricing of Vanilla Options . . . . .                                    | 6         |
| 2.1.2    | Basket Options . . . . .                                                | 7         |
| 2.2      | Lévy Processes . . . . .                                                | 8         |
| 2.2.1    | The Meixner Process . . . . .                                           | 9         |
| 2.3      | Time deformation and time-change . . . . .                              | 12        |
| 2.4      | Mathematical methods . . . . .                                          | 12        |
| 2.4.1    | Monte Carlo Methods . . . . .                                           | 13        |
| 2.4.2    | Quasi-Monte Carlo Methods . . . . .                                     | 15        |
| 2.4.3    | Randomized Quasi-Monte Carlo Methods . . . . .                          | 18        |
| <b>3</b> | <b>Simulations</b>                                                      | <b>21</b> |
| 3.1      | Number Generation . . . . .                                             | 21        |
| 3.2      | Numerical Example . . . . .                                             | 21        |
| 3.3      | Calibration of Model Parameters . . . . .                               | 26        |
| 3.3.1    | The Fourier transform of an option price . . . . .                      | 26        |
| 3.3.2    | Fast Fourier transformation FFT . . . . .                               | 28        |
| 3.3.3    | Calibration Results . . . . .                                           | 28        |
| 3.4      | Simulation Routine . . . . .                                            | 31        |
| <b>4</b> | <b>Results</b>                                                          | <b>33</b> |
| 4.1      | Monte Carlo simulations of the Basket Option . . . . .                  | 33        |
| 4.2      | Quasi-Monte Carlo simulations of the Basket Option . . . . .            | 36        |
| 4.2.1    | Sobol sets for estimating Basket options . . . . .                      | 36        |
| 4.2.2    | Halton sets for estimating Basket options . . . . .                     | 40        |
| 4.3      | Randomized quasi-Monte Carlo simulations of the Basket Option . . . . . | 43        |
| 4.3.1    | Randomized quasi-Monte Carlo Simulation with Sobol sequences . . . . .  | 43        |
| 4.3.2    | Randomized quasi-Monte Carlo Simulation with Halton sequences . . . . . | 46        |
| 4.4      | Model fit to real values . . . . .                                      | 50        |
| <b>5</b> | <b>Conclusions</b>                                                      | <b>51</b> |
| <b>A</b> | <b>Appendix A</b>                                                       |           |
|          | S&P-500 call option prices                                              | <b>56</b> |

## Acknowledgements

This master thesis was written at the department of Mathematical Statistics at Lund Univeristy during the autumn of 2015. It was submitted in fulfillment of the requirements for the degree Master of Science in Industrial Engineering and Management.

I would like to express my deepest gratitudes and thanks to my supervisor Prof. Magnus Wiktorsson for his support, feedback, constructive suggestions and help. I am also very grateful for his help of coming up with a Matlab routine to simulate from the Meixner distribution used in this master's thesis.

Lastly, my sincerest gratitude goes to family and friends for their support both on and off campus during my six years at Lund University.

# 1 Introduction

The idea of option contracts have a long history in commerce since they provide very good mechanisms for risk control. Aristotle wrote that by observing the stars, Thales the Milesian believed that the olive harvest would be very good in the summer and therefore rented olive presses in advance during the winter when the demand was low and hence also the price. When summer came, his beliefs was proven right and by controlling the supply of the equipment while the demand was high, he could make a profit. [22]

Nowadays, options are extremely popular financial instruments. They are often included in portfolios as a hedge or as speculation. The most common types of standard option contracts are European and American options. Also new types of options have arisen in order for investors to create their own preferred risk profile for their portfolios. Since options play a vital part of the financial market they must be priced correctly and there exist several different techniques for pricing options today.

Perhaps the most popular valuation model is the Black & Scholes PDE. This model is commonly used to price European options as there exist an analytic solution for their prices. Although, in most cases of exotic options it is almost impossible to express the BS-PDE in an analytic formula. It has been known for a substantial amount of time now that the standard option pricing model of Black & Scholes is inconsistent with option market data. The Black & Scholes-model leads to simple calculations, which is nice, but are derived under the assumption that the time interval between observations are very small and that the log prices follows a random walk with normally distributed innovations. Further more, according to a random walk model the standard deviation  $\sigma$  of the innovations, i.e. the volatility of the stock price, must remain constant over time. All these assumptions are somewhat unrealistic and leads to discrepancy between theoretical option prices and market prices.

More sophisticated models have been developed during the last couple of decades. Lévy processes were first studied in the 30's as a part of general probability theory for limits of random sequences. In the 90's they became a popular building block in models used in financial mathematics. Multivariate models have become more and more important for option pricing. In particular, the most traded options, the index options, are in principle options on an average of multiple assets. Neglecting correlations between the constituent assets could provide severe mispricings of these options. In this thesis we are going to use a Lévy process called the Meixner process which was first introduced by Shoutens and Teugels [26] in 1998. In order to improve the accuracy of the model we are going to integrate a Cox-Ingersoll-Ross-process, as suggested by Carr, Geman, Madan and Yor in [6], to make business time stochastic to incorporate stochastic volatility in a Lévy process. By using Monte Carlo simulations with the assumed underlying model

the expected value of the option can be estimated. The advantage of using Monte Carlo methods is that it can be adapted to price almost any type of option with the assumed underlying process of our choice. Many financial derivatives are either path-dependent and depends on the state variables or have multiple underlying assets. The payoff function can then be written as a multi-dimensional integral. In these cases, Monte Carlo methods provide a powerful tool to use.

The main drawback of using Monte Carlo methods is that it is computationally demanding and converge rather slow, even for simple vanilla options. However, there are methods to improve the efficiency of the Monte Carlo simulations. One innovation in the area is the usage of quasi-Monte Carlo methods, see e.g. [24]. Instead of using random sequences, deterministic sequences that have favorable properties are being used. In this thesis we are going to use two different deterministic sequences. The first one is called Halton sequences and the second is called Sobol sequences. Although in theory quasi-Monte Carlo seems promising, the major drawback of QMC is that it is very hard to estimate the error of your simulations, since we use deterministic sequences standard statistical error estimation techniques cannot be used.

There is however one trick that can be done. We can randomize the deterministic sequences. That may seem rather counterintuitive that after choosing "good" deterministic sequences start randomizing them but there is at least one major reason for doing this. By randomizing the sequence we open the possibility to estimate the error by statistical techniques while preserving much of the accuracy of pure QMC. This is what we call Randomized quasi-Monte Carlo. There are different methods of randomizing the deterministic sequences. In this thesis we are going to use the so-called Randomly Shifted Low Discrepancy Sequence as proposed by Tuffin in [30].

We are in this thesis going to compare five different Monte Carlo methods for pricing both vanilla options and basket options. First we are going to create a simulation algorithm to generate Meixner distributed random variables in order to create the Meixner Lévy Process. We are further going to implement an integrated CIR-process to determine the length of the time steps. With these two simulation algorithms in place we are going to estimate the option prices with the five different Monte Carlo methods.

In section 2 we describe the theory of both the underlying process as well as the theory of the different Monte Carlo methods used. Next, in section 3 we review the different Monte Carlo methods by using them on a numerical problem with known expected value and we calibrate our market parameters from market data. In section 4 we provide numerical results of the thesis; we compare the different methods in accuracy and speed. Finally in the last section, we provide a conclusion based on the result and suggestions of further research topics related to this work.

## 2 Theory

### 2.1 Pricing of Derivatives

In this section we are going to describe the basic theory of pricing derivatives in the financial market. Before we go in to details we need to make some definitions. Let us define the daily interest rate as  $r$  and we define a fixed planning horizon with  $T$ . We then assume the existence of a risk-free asset and a risky asset. We define the risk-free asset as  $B = B_t = e^{rt}, 0 \leq t \leq T$ , i.e. we receive a sure payoff, driven by the risk-free rate,  $r$  and the time  $t$ . The risky asset's process can be described as  $S = S_t, 0 \leq t \leq T$  where we discuss the dynamics of the chosen process in this thesis in section 2.5.

#### 2.1.1 Pricing of Vanilla Options

With the definitions above we are ready to describe the payoff function of vanilla European call and put options:

$$\begin{aligned}C(K, S_t) &= \max(S_T - K, 0) \\P(K, S_t) &= \max(K - S_T, 0)\end{aligned}$$

where  $K$  is the predefined strike price of the option. As we see, the value of the option is varying depending of the underlying asset at time  $T$  and the chosen strike  $K$ . To price the option correctly, the price must consider the likelihood of finishing in-the-money, i.e. the chance of  $(S_T > K)$  for a call option and  $(S_T < K)$  for a put option.

In order to price the option we are going to take advantage of the Fundamental Theorem of Asset Pricing (see e.g. [10] or [11]) which states that for a stochastic process,  $(S_t)_{t \in \mathbb{R}}$ , the existence of an equivalent martingale measure (a risk-neutral probability measure) is essentially equivalent to the absence of arbitrage opportunities. This means that the arbitrage-free price,  $V_t$ , of our derivative at time  $t \in [0, T]$  is given by

$$V_t = E_Q[e^{-r(T-t)}G(\{S_u, 0 \leq u \leq T\})|\mathcal{F}_t], \quad (1)$$

where the function  $G(\cdot)$  is the payoff function of the derivative, in this case the call or put option. The expectation is in the equivalent martingale measure,  $Q$ , which is a probability measure which has the same null-sets as the given historical probability measure and under the discounted process  $\{e^{-rt}S_t\}$  is a martingale. Note that an equivalent martingale measure is specific to the chosen numeraire and you can choose different numeraires to receive equivalent martingale measures.  $\mathcal{F} = \mathcal{F}_t, 0 \leq t \leq T$  is the natural filtration of  $S_t$ .

According to Haugh [18], a model that is incomplete is a model that has future states that cannot be constructed by existing assets. If a model is incomplete there does not exist one unique equivalent martingale measure. This means that there exists more than one price of each derivative that fulfill the

”no-arbitrage condition”. This topic is discussed by Fritteli in [13] since this can be seen as a problem. If we have an incomplete market one has to take the agent’s own preferences into consideration when pricing the derivative. One may take other principles into consideration as well in order to select a specific martingale measure and accordingly price contingent claims. Since the choice of pricing measure is considered to be outside of the scope of this thesis it will not be discussed further here but for a deeper discussion of the topic, see [13].

All types of vanilla options have some characteristics in common. They all have one underlying asset, the effective starting time is present, only the price of the underlying asset at the maturity date decides the payoff and whether the option is a call or put is known when it is sold. To see a complete list of characteristics in common for the vanilla options, the reader is referred to Zhang’s paper [31]. Due to their lack of flexibility, the vanilla options have many limitations. In order to try to overcome the limitations, so-called exotic options has been developed. Each kind of exotic option aims to overcome at least one limitation of vanilla options (to some degree).

### 2.1.2 Basket Options

As mentioned, the payoff of a vanilla option depends only on one underlying asset value at maturity. In this thesis we are going to be pricing basket options. This type of option is an exotic option whose payoff depends on the value of an arbitrary chosen portfolio of assets. The basket is made out of a weighted sum of  $N$  underlying assets. Options written directly on this portfolio yields an efficient method of hedging the risk of such an exposure. The literature on multiple asset options is somewhat limited according to [4] but there has been work done the last twenty years and in the last couple of years the multivariate models for asset returns have recieved much attention, see [19]. If we denote the basket value at time  $t$  as  $B_t$ , then the value of the basket is given by:

$$B_t = \sum_{i=1}^N w_i S_t^{(i)},$$

where  $w_i$  is the weight of of the coresponding underlying asset,  $S_t^i$  and  $\sum w_i = 1$ . The payoff structure of the basket option is defined by:

$$G_B(T) = \phi \left( \sum_{i=1}^N w_i S_T^{(i)} - K \right)^+, \quad (2)$$

where  $\phi$  equals 1 if it is an call option and -1 if it is an put option. With these options the main problem is not path-dependency but the multidimensionality which makes it impossible to give exact analytical representations of the option prices. There are several different methods that aims to approximate basket options, see [21] for a comparison of different so-called analytical approximations. Recent development in pricing basket options is using asymp-



otic expansion methods, see e.g. [16]. All these methods use Monte Carlo simulations as a measure of "true" option value which indicate to us that there is no preferred superior method for pricing basket options yet. We are in this thesis therefore going to use different Monte Carlo Methods in order to estimate basket option prices, see section 2.4.

## 2.2 Lévy Processes

The underlying process we are going to use in this master thesis is the Meixner Lévy Process. It is therefore appropriate to introduce the reader to basic theory of Lévy processes before we go in to details about the Meixner Process.

We start by defining a set of probability measures on the line as  $\mathcal{P}$ . We can then uniquely determine an element,  $P \in \mathcal{P}$  by its distribution function  $F_P(x) = P((-\infty, x]), x \in \mathbb{R}$  and its characteristic function, which is the Fourier transform of the distribution,  $F_P$ :

$$\varphi(\lambda) = \int e^{i\lambda x} F_P(dx), \quad \lambda \in \mathbb{R} \quad (3)$$

A probability distribution,  $P$ , is called infinitely divisible if and only if, for every integer  $n \geq 1$ , there exists a characteristic function  $\varphi_n$ , such that  $\varphi_P(t) = \varphi_n(t)^n$ .

With a stochastic process we mean a collection of random variables  $X_t, t \in T$  with values in  $\mathbb{R}$  and  $T$  is time, see Knill's notes [20]. If we say that a stochastic process is càdlàg (continu à droite, limites à gauche) we mean that we allow jumps in the process but require that the process is right continuous with probability 1, i.e.

$$\lim_{s \downarrow t} X_s = X_t$$

The process also need to have a limit from the left:

$$X_{t-} = \lim_{s \uparrow t} X_s$$

With these introduced definitions we are now ready to define a Lévy process and describe some characteristics of such processes. A process is called a Lévy process if and only if the càdlàg stochastic process  $X = \{X_t\}, t \geq 0$  with  $X_0 = 0$  has independent and strictly stationary increments. This means that the distribution of an increment over  $[s, s + t], s, t \geq 0$ , i.e.  $X_{s+t} - X_s$  has  $(\varphi(\lambda))^t$  as characteristic function.

When using Lévy processes it is common to talk about the process' triplet of Lévy characteristics. In order to describe this triplet we need to introduce the characteristic exponent, which is defined as:  $\psi(\lambda) = \log \varphi(\lambda)$  and it satisfies the Lévy-Khintchine formula:

$$\psi(\lambda) = i\gamma\lambda - \frac{\sigma^2}{2}\lambda^2 + \int_{-\infty}^{\infty} (\exp(i\lambda x) - 1 - i\lambda x \mathbf{1}_{(|x| < 1)}) \nu(dx), \quad (4)$$

where  $\gamma \in \mathbb{R}$ ,  $\sigma^2 \geq 0$  and  $v$  (*the Lévy measure of  $X$* ) is a measure on  $\mathbb{R} - \{0\}$  such that

$$v(\mathbb{R} - [-1, 1]) < \infty, \text{ and } \int_{-1}^1 x^2 v(dx) < \infty$$

The parameters  $[\gamma, \lambda, v(dx)]$  are the Lévy triplets that are uniquely determined by the specific Lévy process. From Equation 4 above we can distinguish three independent parts that makes it easier to interpret the Lévy triplet.  $\gamma$  is a linear deterministic drift term,  $\lambda$  is a Brownian part and  $v(dx)$  is a pure jump part. The jumps will occur according to a Poisson process with parameter  $\int_A v(dx)$ , where  $A$  is the jump size.

One advantage of using Lévy based models to describe the financial market is that they provide a flexible framework to model the marginal distribution of asset returns. However, using Lévy processes also give us some difficulties. One of the major drawbacks is that the returns will be independent and identically distributed when measured over time intervals of fixed length. Thus stylized facts such as volatility clustering are being ignored by the model. This issue can be resolved and we will discuss a method to deal with this problem in section 2.5.1. Another issue with using Lévy Processes in the financial market that Mazzola and Muliere discuss in their paper [23], is that markets are incomplete when using Lévy processes, i.e. there exist an infinite number of martingale measures equivalent to the physical measure describing the underlying price evolution. This means that each martingale measure corresponds to a set of derivative prices which are compatible with the no-arbitrage requirement; and thus the prices cannot be determined by no arbitrage but instead on every agent's own risk preferences. This means that the derivative prices are determined by particular utility functions, which are different from one agent to another.

### 2.2.1 The Meixner Process

The Meixner distribution belongs to the class of infinitely divisible distributions and as such gives rise to a Lévy Process, called the Meixner Process. The process originates from the theory of orthogonal polynomials proposed in 1998 by Schoutens and Teugels [26]. The density of a random variable  $X$  that has a Meixner distribution,  $MD(\alpha, \beta, \delta, \mu)$ , is given by:

$$f_M(x; \alpha, \beta, \delta, \mu) = \frac{(2 \cos(\beta/2))^{2\delta}}{2\alpha\pi\Gamma(2\delta)} \exp\left(\frac{\beta(x - \mu)}{\alpha}\right) \left| \Gamma\left(\delta + \frac{i(x - \mu)}{\alpha}\right) \right|^2 \quad (5)$$

with  $\alpha > 0$ ,  $\beta \in (-\pi, \pi)$ ,  $\delta > 0$ ,  $\mu \in \mathbb{R}$  and  $\Gamma(\cdot)$  is the Euler Gamma function. The parameter  $\mu$  is a location parameter,  $\alpha$  is a scale parameter and  $\delta$  is a time scale parameter.  $\beta$  is a shape parameter that primarily influencing the skewness of the distribution. The characteristic function of the Meixner distribution is given by:

$$E(\exp(iuX)) = \left( \frac{\cos(\beta/2)}{\cosh(\frac{\alpha u - i\beta}{2})} \right)^{2\delta} \exp(iu\mu) \quad (6)$$

Mazzola and Mulliere has shown in their paper [23] that for the Meixner distribution, moments of all orders exists. The first moment (the mean) is:  $\kappa_1 = \alpha\delta \tan(\beta) + \mu$  and we see that the mean is finite as long as  $\beta \neq \pm\pi$ . The second moment is  $\kappa_2 = \frac{\alpha^2\delta}{1+\cos(\beta)}$  which is also finite as long as  $\beta \neq \pm\pi$ . The skewness of the distribution is:  $\gamma_1 = \sin(\frac{\beta}{2})\sqrt{\frac{2}{\delta}}$  which is finite for all parameter values (except  $\delta = 0$ ). The fourth moment, the kurtosis, is:  $\gamma_2 = 3 + \frac{2-\cos(\beta)}{\delta}$  and we see that the kurtosis is always greater for the Meixner distribution compared to the Normal distribution (which has a kurtosis of 3). This hints us that the Meixner distribution potentially fits financial data better compared to the Normal distribution since the stylized facts of financial data have shown that the distribution of the real data has higher peaks and fatter tails than the normal distribution. If  $X \sim MD(\alpha, \beta, \delta, \mu)$ , then the random variable  $Z = (X - \mu)/\alpha$  has the density function  $MD(1, \beta, \delta, 0)$  via a simple standardization.

Properties of the Meixner Lévy process mostly derives from from the corresponding properties of the Meixner distribution. The characteristic exponent of the Meixner distribution is given by:

$$\psi_{Meixner}(u) = -\log \left( \left( \frac{\cos(\beta/2)}{\cosh(\alpha u - i\beta)/2} \right)^{2\delta} \right) - iu\mu \quad (7)$$

The characteristic Lévy triplet of the Meixner distribution with parameters  $MD(\alpha, \beta, \delta, \mu)$  is  $(\gamma, 0, v(dx))$  where:

$$\gamma = \alpha\delta \tan \frac{\beta}{2} - 2\delta \int_1^\infty \frac{\sinh(\beta x/\alpha)}{\sinh(\pi x/\alpha)} dx + \mu \quad (8)$$

$$v(dx) = \delta \frac{\exp(\beta x/\alpha)}{x \sinh(\pi x/\alpha)} dx \quad (9)$$

For derivation and proof of the Lévy triplets see Shouten's paper [27]. As seen in the Lévy triplet, the Meixner process does not have a Brownian part since  $\sigma = 0$  and hence is a pure jump model. Another property of the Meixner distribution worth mentioning is that if  $X_j \sim MD(\alpha, \beta, \delta_j, \mu_j)$ ,  $j = 1, \dots, n$  and are mutually independent, then:

$$X_1 + \dots + X_n \sim MD \left( \alpha, \beta, \sum_{j=1}^n \delta_j, \sum_{j=1}^n \mu_j \right).$$

The Meixner process  $X = (X_t, t \geq 0)$  is a Lévy process such that:

$$X_t \sim MD(\alpha, \beta, \delta t, \mu)$$

This process is of infinite variation since it can be shown by standard Lévy process theory (see e.g. [3]) that  $\int_{-\infty}^\infty |x|v(dx) = \infty$ . This is called that the model is an infinite activity Lévy process and these models are able to capture

both small frequent movements as well as rare large movements.

In the Meixner Lévy Market Model, which we are going to use in this thesis, we assume that the risky asset is modeled as:

$$S_t = S_0 \exp(MD_t)$$

The log returns,  $\log(S_{t+s}/S_t)$ , follow the distribution of increments of the length  $s$  of the Meixner Process  $MD_t$ . In order to have a price process with finite expected value, the following criteria must be fulfilled by the parameters in the Meixner distribution:  $\alpha + \beta < \pi$  and the process has finite variance if  $2\alpha + \beta < \pi$ .

To find an equivalent martingale measure, we can use the so called Esscher transform that was first proposed by Esscher in 1932 and used by Gerber and Shiu in 1994 for asset pricing in incomplete markets [14]. The idea is to define a new measure,  $Q$  as:

$$Q(dw) = ce^{-X(w)^2} P(dw), \quad w \in \Omega \quad (10)$$

where  $X$  is a univariate random variable on the probability space  $(\Omega, \mathcal{F}, P)$  and such that  $P(X \neq 0) > 0$ . The normalizing constant  $c$  is defined as:  $c = 1/E_P[e^{-X^2}]$ . We now let  $\xi(\theta) = E_Q[e^{\theta X}]$  where  $\theta \in \mathbb{R}$ . Finally we define a new variable as:

$$Z_\theta(w) = \frac{e^{\theta X(w)}}{\xi(\theta)} \quad (11)$$

The mapping of  $x \rightarrow e^{\theta x}/\xi(\theta)$  is what we call the Esscher transform with parameter  $\theta$ . By changing our P-measure to the Q-measure (the risk-free measure) via the Esscher transform, our Meixner distribution goes from  $MD(\alpha, \beta, \delta, \mu)$  to  $MD(\alpha, \alpha\theta + \beta, \delta, \mu)$ , where  $\theta$  is the unique Esscher transform parameter for the Meixner distribution. If we specify  $\beta_Q$  as the solution to the equation:

$$\cos\left(\frac{\beta_Q}{2} + \frac{\alpha}{2}\right) = \exp((\mu - r)/(2\delta)) \cos\left(\frac{\beta_Q}{2}\right) \quad (12)$$

where the solution is given by:

$$\beta_Q = 2 \arctan\left(\frac{(\cos(\frac{\alpha}{2}) - \exp((\mu - r)/(2\delta)))}{\sin(\frac{\alpha}{2})}\right) \quad (13)$$

we see that  $\beta_Q$  always fulfill the requirement of  $|\beta| < \pi$ . The unique Esscher transform parameter can be derived from the fact that the new  $\beta$ -parameter is defined as  $\beta_Q = \alpha\theta + \beta_P$  and Equation 13. This gives us the equation:

$$\theta = \frac{\beta_Q - \beta_P}{\alpha} \quad (14)$$

In this case, the Esscher transformed Meixner model incorporate by itself a volatility smile effect. Although, the smile effect is not enough and distinct differences between market prices and model prices still exist. We need to correct the model for this issue.

### 2.3 Time deformation and time-change

The main feature the above described Meixner Lévy process is missing is the fact that volatility is changing stochastically over time. Empirical financial data shows that estimated volatilities tend to be clustered with some periods with high absolute log-returns and some periods with lower absolute log-returns, see [27]. This phenomenon of volatility clustering can be incorporated in the model by making the time stochastic. There are different methods for choosing a time change which is suitable for financial modeling. Two popular classes are subordinators and absolutely continuous time changes and sometimes the terms are used synonymously in finance literature according to [1]. In this thesis we are going to use an absolutely continuous time-change. This class is of the form  $T_s = \int_0^s \tau_u du$ , for a positive and integrable process  $\tau = (\tau_s)_{s \geq 0}$ . In this setting  $T$  is always continuous but  $\tau$  can exhibit jumps. The process  $\tau$  is often called instantaneous (business) activity rate. One advantage of this class is that it leads to affine models which are highly analytically tractable in contrast to stochastic integrals with respect to Lévy processes which in general are not affine.

In this thesis we are using a process proposed by Carr, Madan, Geman and Yor in [6]. In order to build volatility clustering and to keep time going forward we have a mean-reverting positive process as a measure of the local time change rate. In this particular case we use the Cox-Ingersoll-Ross-process (CIR-process)  $y(t)$  that solves the stochastic differential equation:

$$dy_t = \kappa(\eta - y_t)dt + \lambda y_t^{1/2} dW_t \quad (15)$$

where  $W_t$  is a Wiener process,  $\kappa \geq 0$  corresponds to the speed of adjustment,  $\eta$  is the mean and  $\lambda$  is the volatility. The economic time elapsed in terms of calendar time is then given by  $Y(t)$  where:

$$Y(t) = \int_0^t y_s ds \quad (16)$$

The characteristic function of  $Y(t)$  have been shown by e.g. Carr et al. in [6] to be:

$$E(\exp(iuY(t))) = \phi(u, y) = \frac{\exp(\kappa^2 \eta t / \lambda^2) \exp(2y(0)iu / (\kappa + \gamma \coth(\gamma t / 2)))}{(\cosh(\gamma t / 2) + \kappa \sinh(\gamma t / 2) / \gamma)^{2\kappa \eta / \lambda^2}}, \quad (17)$$

where

$$\gamma = \sqrt{\kappa^2 - 2\lambda^2 i u}. \quad (18)$$

### 2.4 Mathematical methods

In the following section the theory behind the mathematical methods used in this thesis are presented. There will be a brief introduction to Monte Carlo methods, Quasi-Monte Carlo methods and lastly an introduction to randomized quasi-Monte Carlo methods.

### 2.4.1 Monte Carlo Methods

Monte Carlo methods is a technique where you use computational algorithms to repeatedly generate random numbers to solve a problem. A narrower definition was stated by Halton [17]: "the Monte Carlo methods are defined as representing the solution of a problem as a parameter of a hypothetical population, and using a random sequence of numbers to construct a sample of the population, from which statistical estimates of the parameter can be obtained".

A common application of Monte Carlo methods is to estimate integrals, see e.g. [28]. Consider the integral:

$$\tau = E(\phi(X)) = \int \phi(x)f(x)dx \quad (19)$$

here  $\phi : \mathbb{R}^d \rightarrow \mathbb{R}$ ,  $X \in \mathbb{R}^d$  and  $f$  is the probability density of  $X$ . The probabilities can be rewritten as  $\phi$  being an indicator function:

$$P(X \in A) = \int \mathbb{1}\{x \in A\}f(x)dx \quad (20)$$

Now, by using the Law of Large Numbers (LLN), an approximation of  $\tau$  can be achieved according to the equation:

$$\tau_N = t(x_1, \dots, x_N) = \frac{1}{N} \sum_{i=1}^N \phi(x_i) \quad (21)$$

where  $x_1, \dots, x_N$  are independently drawn from  $f$ . As we see the LLN can be interpreted as a statement that the Monte Carlo estimate of an integral is (under certain conditions) a consistent estimate, i.e. it converges to the correct value as the random sample size becomes larger. If we further assume that  $\phi$  is square integrable we can calculate the variance as:

$$\sigma_f^2 = \int (\phi(x) - \tau)^2 dx \quad (22)$$

The Central Limit Theorem asserts that the estimation error ( $\tau - \tau_N$ ) is approximately normally distributed with zero mean and standard deviation  $\sigma_f/\sqrt{N}$ . This is often written in literature as:

$$\frac{\tau_N - \tau}{\sigma_f\sqrt{N}} \rightarrow N(0, 1) \quad (23)$$

This feature is nice in theory but in practice if  $\tau$  is unknown typically one can assume that also  $\sigma_f$  is unknown. This issue can be solved by estimating the sample standard deviation instead:

$$s_f = \sqrt{\frac{1}{N-1} \sum_{i=1}^N (\phi(x_i) - \tau_N)^2} \quad (24)$$

The standard error is therefore of convergence rate  $O(N^{-1/2})$ . This is considered a rather slow rate of convergence compared to other classical quadrature rules for smooth functions in low dimensions (see [9]). The value of using Monte Carlo methods is the fact that the convergence rate does not depend on the dimension  $d$ ! In addition, if we have a finite but at least moderately large  $n$ , we can also estimate a confidence interval of the point estimate,  $\tau_N$  as:

$$\tau_N \pm z_{\delta/2} \frac{s_f}{\sqrt{N}} \quad (25)$$

where  $z_{\delta/2}$  denotes the  $(1 - \delta)$ -quantile of the standard normal distribution. This is justified by the Central Limit theorem and is an asymptotically confidence interval.

One way to increase the efficiency of Monte Carlo simulation is to use variance reduction techniques [15]. One example is to use a technique called antithetic variates which attempts to reduce the variance by using negative dependence between replication pairs. Lets assume we want to estimate  $\tau$  with an error less than a given constant,  $\epsilon > 0$  from the expression of the confidence interval in Equation 25 we see that:

$$z_{\delta/2} \frac{s_f}{\sqrt{N}} < \epsilon \iff N > z_{\delta/2}^2 \frac{s_f^2}{\epsilon^2} \quad (26)$$

i.e. the sample size  $N$  increases lineary with the variance  $s_f^2$ . When using antithetic variables we are going to assume we can generate another variable,  $Y$  that also has  $\tau$  as expected value and the same variance as  $X$ . We can then define a third variable,  $Z$  as:

$$Z = \frac{X + Y}{2} \quad (27)$$

also with  $\tau$  as expected value and with variance:

$$\begin{aligned} Var(Z) &= Var\left(\frac{X + Y}{2}\right) = \frac{1}{4}(Var(X) + 2Cov(X, Y) + Var(Y)) \\ &= \frac{1}{2}(Var(X) + Cov(X, Y)) \end{aligned} \quad (28)$$

For a desired size of the estimation error,  $\epsilon$ , it is better to use  $Z$  if:

$$\begin{aligned} 2z_{\delta/2} \frac{Var(Z)}{\epsilon^2} &< z_{\delta/2} \frac{Var(X)}{\epsilon^2} \iff \\ Var(X) + Cov(X, Z) &< Var(X) \iff \\ Cov(X, Z) &< 0 \end{aligned} \quad (29)$$

This means that if we can find a variable  $Y$  that is negatively correlated with our original variable  $X$  we would increase the efficiency of the Monte Carlo simulation.

### 2.4.2 Quasi-Monte Carlo Methods

Another way of increasing the efficiency of the Monte Carlo simulation is to consider using deterministic sequences instead. The discussion in this section is mainly based on the work of Niederreiter in [24]. It can be shown that it is not so much the true randomness of the sampling that is relevant but rather that the samples should be spread in a uniform manner over the integration domain in order to increase accuracy of the estimation. This leads to the idea of selecting deterministic nodes in such a way that the error bound is as small as possible instead. This is the fundamental principle of Quasi-Monte Carlo methods (QMC). We try in no way to mimic randomness but rather choose "good" points instead. The tools and theory that QMC is based on are very different from those that are being used in ordinary Monte Carlo. QMC theory is based on number theory and abstract algebra compared to MC that is based on probability and statistics theory. We will go through the main ideas of QMC in the following section and refer the reader to [24] for a thorough explanation of the theory.

Since QMC is a completely deterministic procedure it implies that we get deterministic and thus guaranteed error bounds. In principle this means that it is possible to determine in advance an integration rule that yields a prescribed level of accuracy. We need to replace the random samples from ordinary Monte Carlo by well-chosen deterministic points. The selection criterion is based on uniformly distributed sequence and discrepancy. The discrepancy can be seen as a quantitative measure for the deviation from uniform distribution.

If we want to estimate the integrand,  $f$ , we use the QMC approximation:

$$\int_{I^d} f(u) du \approx \frac{1}{N} \sum_{i=1}^N f(x_n) \quad (30)$$

where  $I^d := [0, 1)^d$ , is the half-open  $d$ -dimensional unit cube and  $x_1, x_2, \dots, x_N \in I^d$ . It can be shown that the desirable nodes are those for which the empirical distribution is close to the uniform distribution on  $I^d$ , i.e. the nodes  $x_1, \dots, x_N$  should be evenly distributed over  $I^d$ . Let us define discrepancy more detailed. For  $N$  points  $x_1, x_2, \dots, x_N \in I^d$  and  $J$  as a collection of subsets of  $I^d$ , if  $A(J)$  counts the number of points  $x_i \in I^d$  and  $V(J)$  is the volume of  $J$ , we define the discrepancy  $D(J, N)$  as:

$$D(J, N) = \left| \frac{A(J)}{N} - V(J) \right| \quad (31)$$

Intuitively, the discrepancy is the difference between the proportion of points in  $J$  compared to the full unit cube  $I^d$ . If we take  $J$  to be the collection of rectangles in  $I^d$  in the form:

$$\prod_{j=1}^d [u_j, v_j), \quad 0 \leq u_j < v_j \leq 1, \quad (32)$$



we get the ordinary discrepancy but if we instead restricting  $J$  to the rectangles of:

$$\prod_{j=1}^d [0, u_j) \quad (33)$$

we get what is defined as the star discrepancy  $D^*(x_1, \dots, x_N)$  which is no larger than the ordinary discrepancy. Niederreiter shows in [24] that in dimension,  $d = 1$ :

$$D^*(x_1, \dots, x_n) \geq \frac{1}{2N}, \quad D(x_1, \dots, x_N) \geq \frac{1}{n} \quad (34)$$

which in both cases yields the minimum if:

$$x_i = \frac{2i-1}{2N}, \quad i = 1, \dots, N \quad (35)$$

The problem is though that much less is known about the best discrepancy in higher dimensions. Niederreiter uses the expression "it is widely believed" to state that in  $d \geq 2$ , any points  $x_1, \dots, x_N$  satisfy:

$$D^*(x_1, \dots, x_N) \geq c_d \frac{\log(N)^d}{N} \quad (36)$$

where  $c_d$  is a constant dependent on the dimension  $d$ . There is no proof of whether this is correct or not. The goal of a low-discrepancy sequences (LDS) is to minimize this star discrepancy, see [8]. In other words, LDS are numbers that are better equidistributed in a given volume than random numbers.

Simulations of QMC with LDS can potentially achieve faster convergence and better accuracy than standard Monte Carlo methods. Since the points in a LDS are deterministic there are correlation between the points to eliminate clumping of points. But because of the correlation, LDS are less versatile than random sequences.

With the notation above we can now describe the integration error bound,  $\epsilon$  of QMC:

$$\epsilon(f) \leq V(f)D_N^* \quad (37)$$

where  $f$  is any function with finite Hardy-Krause variation. This is known as the Koksma-Hlawka bound. Note that when using QMC we only have an (theoretical) upper bound of the integration error and we cannot exactly estimate the real error as we can in the ordinary MC case. A comparison of the error bound of standard MC and the Koksma-Hlawka inequality in QMC are stated below and are discussed by Caflisch in [5].

- The Koksma-Hlawka inequality in Eq. 37 is a worst-case strict bound, whereas Eq. 25 is a probabilistic bound dependent on  $n$ .
- The two terms in Eq. 37 are very difficult to compute, in some cases even harder than the integral  $f$  itself. Whereas the variance in standard Monte Carlo is easily estimated.

- In cases where both terms  $V(f)$  and  $D_N^*$  in Eq. 37 are known, numerical computation shows that the bound is usually a gross over-estimate of the true error. While the CLT asserts a sound and relatively informative measure of the error in Monte Carlo estimations.
- The condition that the Hardy-Krause variation must be finite,  $V(f) < \infty$  put on a restriction that is unmatched in Monte Carlo estimations. If Hardy-Krause variation is finite it implies that  $f$  is bounded which is not always the case in option pricing.

From Eq. 36 we see that the rate of convergence for QMC is of order  $O((\log(N))^d N^{-1})$  which is much faster for problems in relatively low dimensions compared to the convergence rate of standard MC. Note though that one drawback of QMC compared to MC is the dependence of the level of dimension. To what dimension is QMC appropriate then? Authors of this topic are not unanimous. Some are putting the upper level at 40 dimension while other putting the limit as low as twelve or 15 dimensions. Numerical experimentations of QMC applied to financial problems have found QMC to be effective in even higher dimensions than 40 as well, see e.g. [15].

Another drawback of quasi-Monte Carlo methods is the loss of versatility compared to Monte Carlo methods. Low discrepancy sequences are numbers between 0 and 1 which limits the use of QMC to numerical inversion methods for sampling from the distribution. While there are many different methods to sample from the wanted distribution for ordinary Monte Carlo simulations, e.g. rejection sampling and importance sampling. One shortcoming in this master thesis is that we are not going to compare the efficiency and speed of different simulation methods of the Monte Carlo method with the quasi Monte Carlo and randomized quasi Monte Carlo methods. All distribution samplings are going to be with the inversion method. The problem of comparing different sampling methods is left to other master theses.

There are several different ways to create a LDS. Some examples are Halton Sequences, Sobol Sequences and Niederreiter Sequences, see [8]. Earlier work with QMC has shown that the efficiency of the estimation can differ depending on chosen LDS. Therefore we are going to use two different LDS in this thesis for comparison, namely the Halton Sequence and the Sobol sequence. MatLab has built-in methods to generate both Halton and Sobol sequences but a brief theoretical description of how to generate the sequences are presented below:

The Halton sequence is a generalization of the Van der Corput sequence to higher dimensions. Each dimension is represented in a different prime base  $b$  e.g. (2, 3, 5, 7, ..). To generate the  $n$ -th point in the sequence, consider the base  $b$ -ary expansion of a  $n : \sum_{i=1}^{\infty} a_i b^i$  where the  $b$ -ary coefficients  $a_i \in \{0, \dots, b-1\}$ . The  $n$ -th Halton point  $H(n)$  is the radical-inverse function in base  $b$ , defined as:  $H(n) = \sum_{i=1}^{\infty} a_i b^{-i-1}$ . Even though standard Halton

sequences perform well in low dimensions, correlation problems have been noted between sequences generated from higher primes. For example if we start with the primes 17 and 19 to generate a Halton sequence in  $(0, 1) \times (0, 1)$  in  $\mathbb{R}^2$ , the first 16 pairs of points have perfect linear correlation. To avoid this, it is common to skip the first 20 entries or some other predetermined number depending on the primes chosen. Another solution to this problem is to use so called scrambled Halton sequences, which uses permutations of the coefficients used in the construction of the standard sequence.

Just like Halton sequences, the Sobol sequence starts from the Van der Corput-sequence. Sobol is exclusively in base 2. The coordinates in a  $d$ -dimensional Sobol sequence are permutations of segments in the Van der Corput-sequence. These permutations are created by multiplying binary expansions of consecutive integers by a set of  $d$  numbers of predetermined generator matrices. These generator matrices are created in a certain way for the Sobol sequences. How this matrices are created are outside the scope of this thesis and the reader is referred to [8] or [15] for further explanation of the low-discrepancy sequences.

### 2.4.3 Randomized Quasi-Monte Carlo Methods

One of the main problems with QMC, as mentioned above is that the sample error is often very difficult to estimate. Theoretically, an upper bound can be estimated but it is far from possible in all cases. One way to solve this problem is to use so-called randomized Quasi-Monte Carlo, RQMC. If we use a randomization technique on the deterministic points in the QMC it allows us to use CLT to estimate the error. We try to get the best out of two worlds, we keep the accuracy of QMC and receive a tool to estimate a confidence interval of the error by using randomization. One could say that using RQMC becomes a trade-off between sacrificing some of the precision in order to get a better estimate of the error. Just as in the QMC case, one of the major drawbacks of RQMC is that the method is only applicable when using inversion methods for sampling from the distribution.

There are different randomization techniques that can be used, see e.g. [32]. In this thesis we are going to use Shifted LDS, as described in [30]. Let  $X$  be a random variable that is uniformly distributed over the unit hypercube  $[0, 1]^d$ . We further denote a low-discrepancy sequence as  $(\xi^{(n)})_{n \in \mathbb{N}}$ . With these notations we create a new random variable,  $Z$ , defined as:

$$Z = \frac{1}{N} \sum_{i=1}^N f(\{X + \xi^{(n)}\}) \quad (38)$$

as seen, we now have a deterministic part and a random part. The notation  $\{X + \xi^{(n)}\}$  means that we add the random number  $X$  to each of the values in the sequence  $\xi^{(n)}$  and then use the operator modulo 1 to ensure values between 0 and 1. The idea is now to re-simulate this estimation of  $Z$ ,  $I$

number of times, i.e. we create  $I$  independent copies  $Z_i$  of  $Z$ . We can now use the Central Limit theorem, just as in ordinary Monte Carlo, to estimate the expected value of  $f(X)$ :

$$E(f(X)) \approx \frac{1}{I} \sum_{i=1}^I Z_i \quad (39)$$

The rate of convergence for randomized quasi-Monte Carlo methods depends on some characteristics of the function  $f$ , see [12]. We assume that  $f$  has a bounded variation  $V(f)$  in the sense of Hardy-Krause. If we further can assume Owen's mild smoothness condition holds;  $f$  has a Lipschitz-continuous  $d$ -fold mixed partial derivative on  $[0, 1]^d$  (see Owen's paper [25] for a more detailed explanation), this condition implies that  $f$  in fact has bounded variation on  $[0, 1]^d$ . The rate of convergence of RQMC is then:

$$\text{Var}(f(X)) = O(N^{-3}(\log(N))^{d-1}) \quad (40)$$

If the smoothness condition does not hold, the (asymptotic) variance of RQMC with shifted LDS have been shown by Tuffin [29] and the reader is referred to his paper for the proof:

$$\text{Var}(f(X)) = O(N^{-2}(\log(N))^{2d}) \quad (41)$$

which is significantly better than for standard MC in low dimensions. Empirical tests have although shown that the convergence rate is not always speeded up using the shifted discrepancy sequences compared to standard MC see e.g. [30].

To compare the efficiency of the estimation with RQMC compared to standard MC, we have to use the same total number of simulations. We have to compare the variance of Eq. 39 with the variance of standard MC simulation in Eq. 24 with  $N \cdot I$  random variables. The variance estimation of RQMC is:

$$\begin{aligned} \sigma_{RQMC}^2 &= \frac{1}{I-1} \sum_{i=1}^I \left( Z_i - \frac{1}{I} \sum_{l=1}^I Z_l \right)^2 \quad (42) \\ &= \frac{1}{I-1} \sum \left( \frac{1}{N} \sum_{j=1}^N f(\{X_i + \xi^{(j)}\}) - \frac{1}{I} \sum_{l=1}^I \left( \frac{1}{N} \sum_{n=1}^N f(\{X_l + \xi^{(n)}\}) \right) \right)^2 \\ &= \frac{1}{(I-1)N} \sum_{i=1}^I \left( \sum_{j=1}^N f(\{X_i + \xi^{(j)}\}) - \frac{1}{I} \sum_{l=1}^I \left( \sum_{n=1}^N f(\{X_l + \xi^{(n)}\}) \right) \right)^2 \end{aligned}$$

If we compare this with the variance estimate of the standard Monte Carlo variance estimation (the square of Eq. 24) with  $N_{tot} = N \cdot I$  simulations, we

see that we get a smaller variance if and only if:

$$\sigma_{MC}^2 = \frac{1}{NI-1} \sum_{i=1}^{NI} \left( f(X_i) - \frac{1}{NI} \sum_{j=1}^{NI} f(X_j) \right)^2 > \quad (43)$$

$$\frac{1}{(I-1)N} \sum_{i=1}^I \left( \sum_{j=1}^N f(\{X_i + \xi^{(j)}\}) - \frac{1}{I} \sum_{l=1}^I \left( \sum_{n=1}^N f(\{X_l + \xi^{(n)}\}) \right) \right)^2 = \sigma_{RQMC}^2$$

### 3 Simulations

We now have enough theory to describe the assumptions for the simulations in this thesis and the mathematical methods we are going to compare. First we are going to take a closer look at the different techniques of number generation used in the stock simulations. Secondly we are going to try the different Monte Carlo simulations methods on a stochastic function with known expected value to see the efficiency of the different estimation methods. At the end of this chapter we are going to calibrate our model to fit market data using fast Fourier transformations.

#### 3.1 Number Generation

Both Monte Carlo methods and quasi Monte Carlo methods aims to approximate an integral over the unit cube by selecting a set of points. The difference is how you pick the point set. In Monte Carlo methods the points are independent and identically distributed uniform random vectors from the unit cube while in quasi-Monte Carlo one aim to chose points that are more evenly distributed than random methods. To see the difference in choosing points, all five methods have been used to generate 1000 2-dimensional points and are presented in Figure 1. From the figure we do notice that the Halton points and the Sobol points look more well distributed in  $\mathbb{R}^2$  than the 1000 (pseudo)random points. The 1000 Halton and the 1000 Sobol points are the first 1000 2d-Halton and 2d-Sobol points generated by Matlab respectively. The randomized Halton points, aswell as the 1000 randomized Sobol points are generated through a shift of the LDS with 1000 (pseudo)random numbers uniformly distributed in  $[0,1]$ .

#### 3.2 Numerical Example

Since the purpose of this thesis is to compare different Monte Carlo methods for pricing different kinds of options the efficiency of the methods are crucial but since there exist options without known exact pricing formula one idea is to evaluate the efficiency of the methods on a function with known expected value. We will test the methods on a function of a univariate stochastic variable with known expected value. By doing this we can fairly easy compare the methods and how fast they converge to the correct value. Therefore we are going to use the five methods to estimate  $e^X$  where  $X \sim N(1, 9)$ . This stochastic function has known expected value and variance. The expected value of  $e^X$  when  $X$  is normal distributed is:  $e^{\mu+\sigma^2/2}$ , which in this case is:  $e^{1+9/2} = e^{5.5} \approx 244.69$ . The variance of the function can be calculated from the definition of variance. If we let  $Y = e^X$  then we know that  $Var(Y) = E(Y^2) - E(Y)^2 = E(e^{2X}) - e^{2 \cdot 5.5} = e^{2\mu+4\sigma^2/2} - e^{11} = e^{2+2 \cdot 9} - e^{11} = e^{20} - e^{11} \approx 4.85 \cdot 10^8$ . We notice that this rather simple function has a huge variance which will really test the Monte Carlo methods' rate of convergence. All the random numbers are generated with the inversion method. Figures 2-4 display the

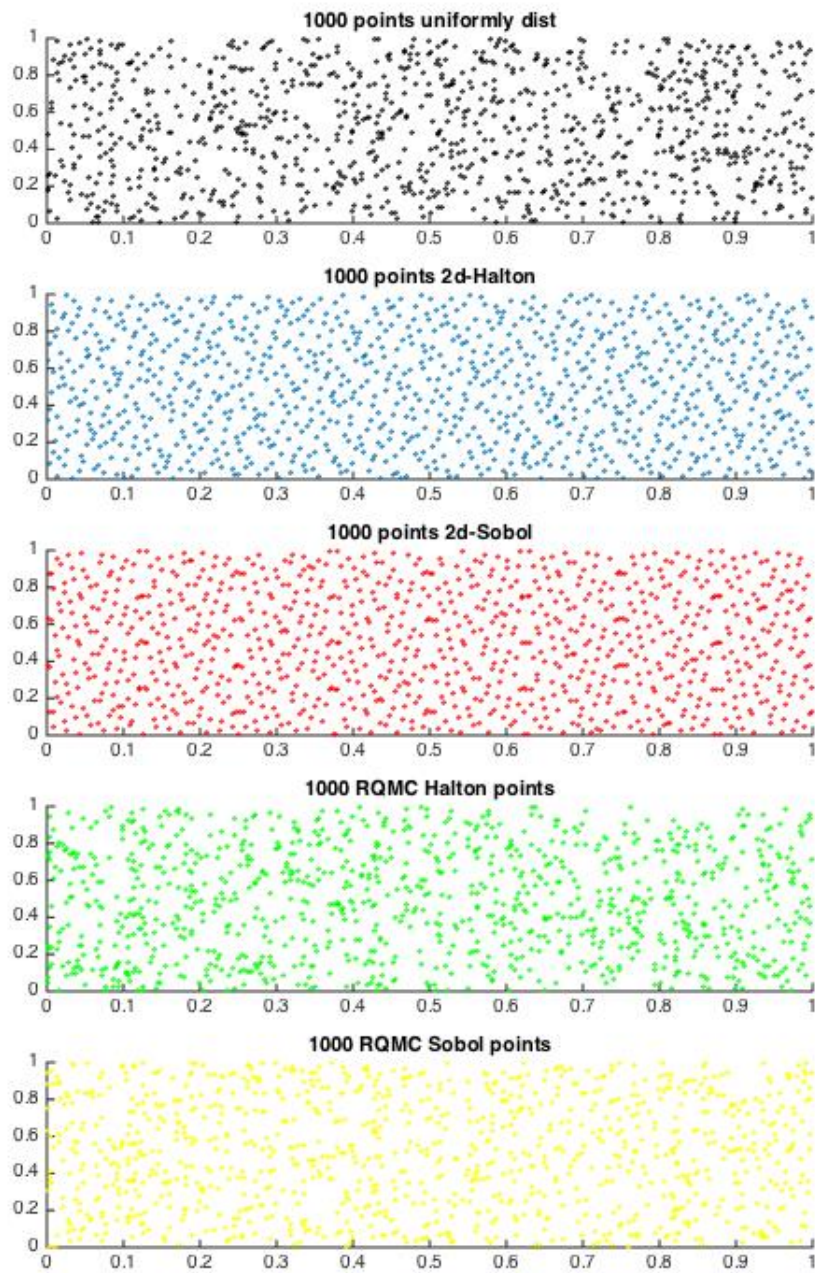


Figure 1: *The five different number generation techniques of generating 1000 2d-points*

standard Monte Carlo method, the two quasi-Monte Carlo methods and lastly the randomized quasi Monte Carlo method with Sobol points.

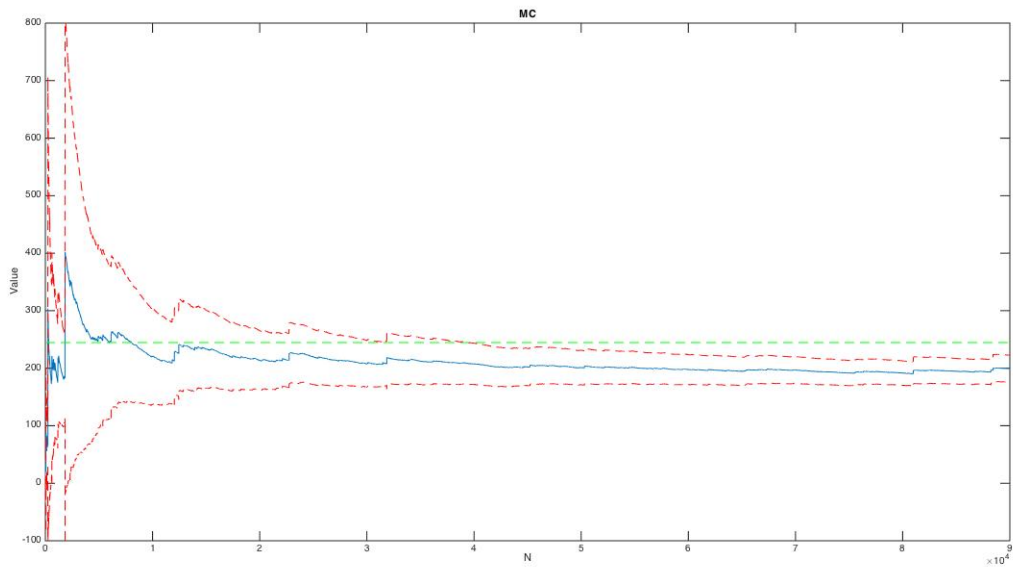


Figure 2: *Standard Monte Carlo estimation of  $e^X$*

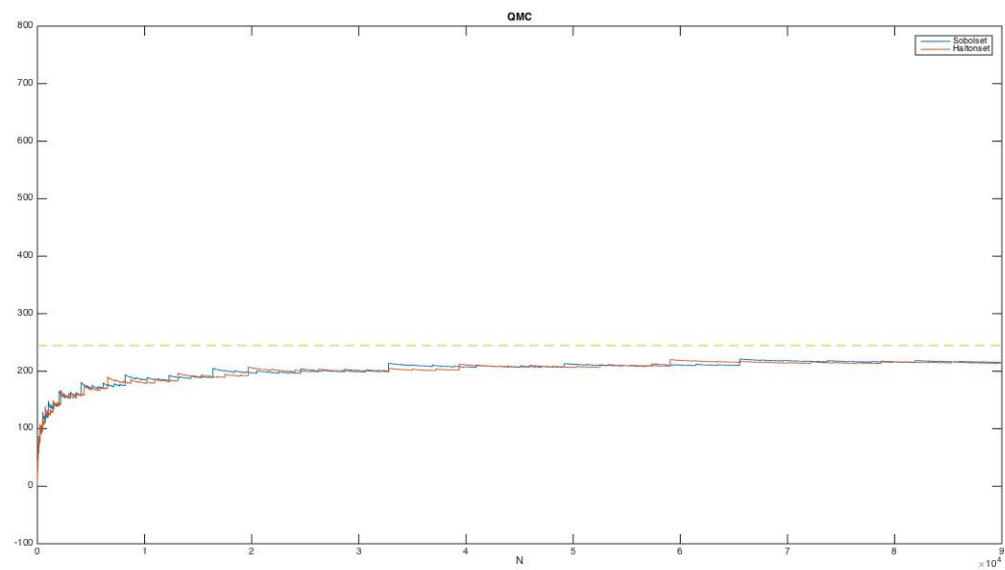


Figure 3: *Quasi-Monte Carlo estimation of  $e^X$  with Halton and Sobol sequences*



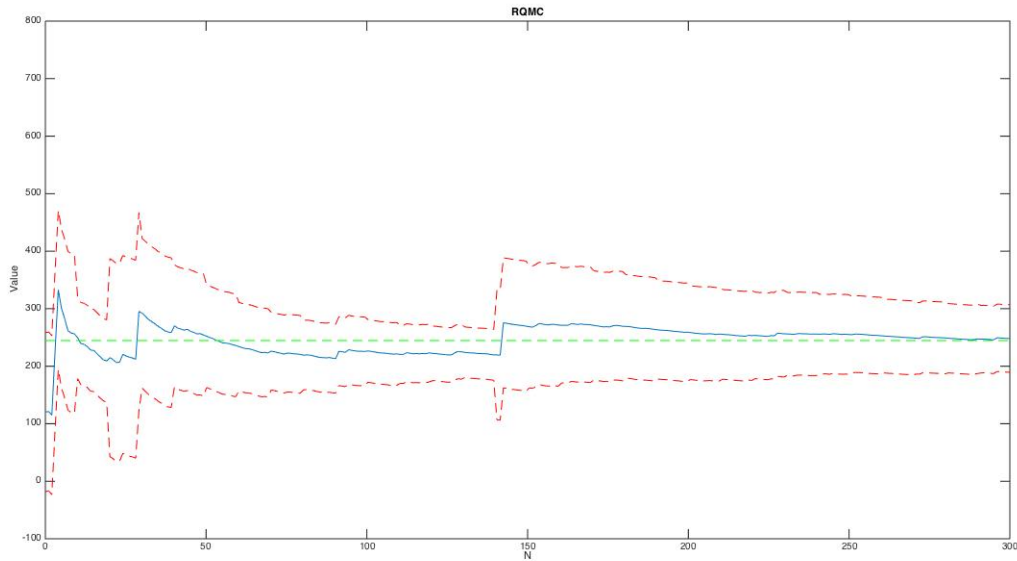


Figure 4: *Randomized quasi Monte Carlo estimation of  $e^X$  with a Sobol sequence*

What we can observe is that the crude Monte Carlo method converges slowly compared to the other methods. In total there are 90000 simulations for every method. Not even after 90000 simulations has the 95%-confidence interval start to cover the true expected value for the crude Monte Carlo simulation. The 95%-confidence intervals are displayed as the dashed lines in the figures. In the randomized quasi Monte Carlo simulation the total number of iterations is 90000 where  $N = 300$  and  $I = 300$ . In figures 5-6 the absolute error of the estimation is displayed for the different methods. After 90000 simulations the absolute errors of the different methods were:

$$\begin{aligned}\epsilon_{MC} &= 45.0240 \\ \epsilon_{QMCH} &= 30.4853 \\ \epsilon_{QMCS} &= 29.4271 \\ \epsilon_{RQMCS} &= 3.3783\end{aligned}$$

As seen both from the numerical values of the error and from the figures, the randomized quasi-Monte Carlo method yields the smallest absolute error and is close to the true value almost immediately. This numerical example tells us that randomized quasi-Monte Carlo methods looks very promising as a method to estimate an expected value. One issue that isn't considered in this example is the effect the dimension of the problem has on the estimation. This example is a low dimensional problem whereas financial problems often are of very high dimensions.

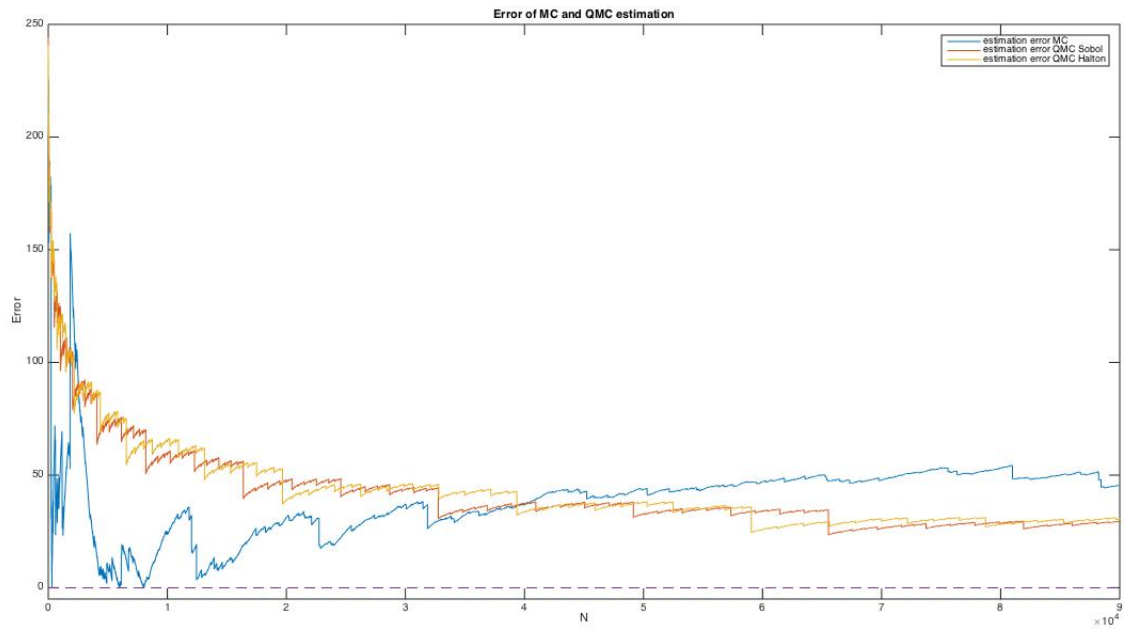


Figure 5: *Absolute error of the Monte Carlo and quasi Monte Carlo simulations*

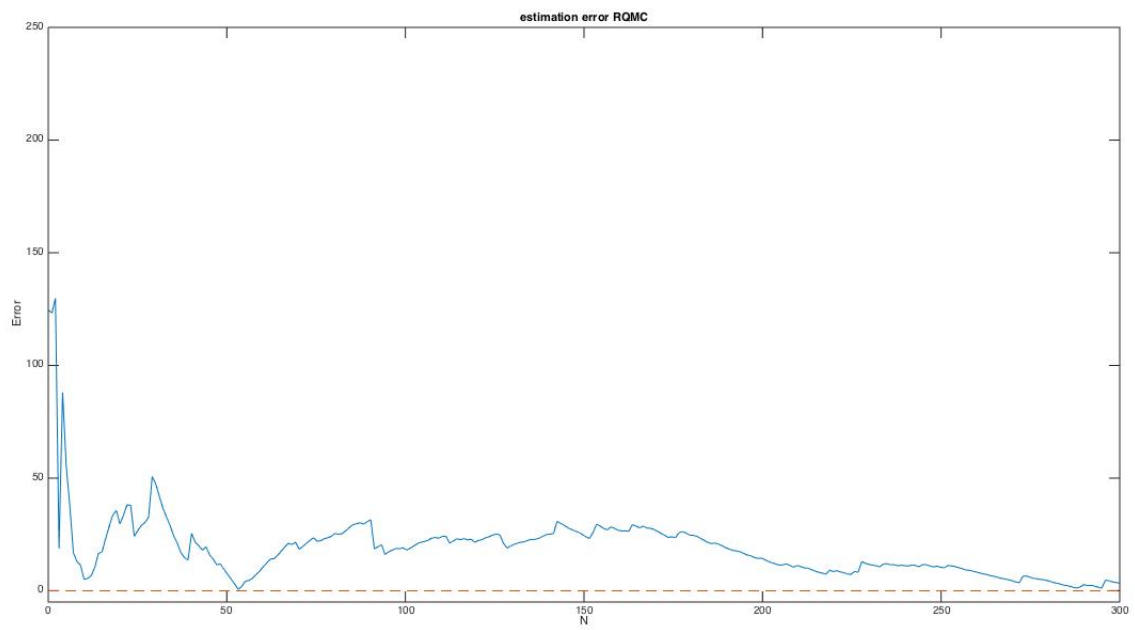


Figure 6: *Absolute error of the randomized quasi Monte Carlo simulation with one-dimensional Sobol points*

### 3.3 Calibration of Model Parameters

The underlying stock price process is assumed to be a Meixner Lévy Process with Esscher transformed parameters to get an equivalent martingale measure. The choice of using a Meixner process in this thesis is due to the fact that the Meixner distribution fits financial data better than the normal distribution used in the Black-Scholes model and the Meixner process is flexible to work with and leads to numerically tractable formulas. Since earlier work have shown that using Lévy processes to simulate financial data don't take stochastic volatility in the data into consideration, an integrated CIR-process is used to make business time stochastic. By making business time stochastic it aims to mimic the effect of volatility clustering of the stockpath. The stock price process used is described in Eq. (44).

$$S_t = S_0 \exp(X_{Y(t)}) \quad (44)$$

where  $X_{Y(t)}$  is the Esscher transformed Meixner Lévy process, where the log returns,  $\log(S_{t+s}/S_t)$ , has the distribution  $MD(\alpha, \alpha\theta + \beta_P, \delta, \mu)$  where  $\theta$  is the Esscher transform parameter.  $Y(t)$  is the integrated CIR-process to make time change stochastic. The characteristic function for the logarithm of our stock price is given by:

$$E(\exp(iu \log(S_t))) = \exp(iu((r-d)t + \log(S_t))) \frac{\phi(-i\psi_X(u), t)}{\phi(-i\psi_X(-i), t)^{iu}}, \quad (45)$$

where  $\phi$  is the characteristic function of the CIR-process described in Eq. (17) and  $\psi_X$  is the characteristic exponent of our Meixner Lévy process described in Eq. (7). See [27] for derivation and proof of the characteristic function of the logarithm of our stock price.

For general Lévy process models we typically cannot find analytical solutions for the European option prices such as we can in the Black & Scholes framework. Therefore, we are going to introduce a pricing method based on the characteristic function of the process in order to calibrate our model parameters. We are going to use fast Fourier transformation FFT, as proposed by Madan and Carr in [7]. Here we will briefly going through the methodology in the following sections.

#### 3.3.1 The Fourier transform of an option price

If we want to evaluate a European call option which are written on a price process  $S_t$  with maturity time  $T$  and strike price  $K$  we start by denoting  $k = \log(K)$  and  $s(T) = \log(S_T)$ . We further denote  $C_T(k)$  as the option price and  $q_T$  the risk-neutral probability density function of the log price,  $s_T$ . The characteristic function of the density function,  $q_T$ , is then:

$$\phi_T(u) = \int_{-\infty}^{\infty} e^{ius} q_T(s) ds \quad (46)$$

The option price related to the risk-neutral density  $q_T$  is then given by:

$$C_T(k) = \int_k^\infty e^{-rT} (e^s - e^k) q_T(s) ds \quad (47)$$

There is one problem though with the equation above.  $C_T(k)$  is not square integrable since when  $k \rightarrow -\infty$  which means that  $K \rightarrow 0$ , we have  $C_T \rightarrow S_0$ . Carr and Madan [7] suggest a modified price  $c_T(k)$  instead in order to achieve a square integrable function:

$$c_T(k) = e^{ak} C_T(k), \quad (48)$$

for a suitable  $a > 0$ . The value of  $a$  will affect the speed of convergence. The Fourier transform of  $c_T(k)$  is given by:

$$\psi(v) = \int_{-\infty}^\infty e^{ivk} c_T(k) dk, \quad (49)$$

and the corresponding inverse Fourier transform is then:

$$c_T(k) = \frac{1}{2\pi} \int_{-\infty}^\infty e^{-ivk} \psi_T(v) dv \quad (50)$$

With Eq. (48) - (50) we can express the option price  $C_T(k)$  as follows:

$$C_T(k) = \frac{\exp(-ak)}{2\pi} \int_{-\infty}^\infty e^{-ivk} \psi_T(v) dv = \frac{\exp(-ak)}{\pi} \int_0^\infty e^{-ivk} \psi_T(v) dv, \quad (51)$$

where we in the last equation used the fact that  $T$  is odd in its imaginary part and even in its real part and we know that  $C_T(k)$  is real. Now, lets express the Fourier transform,  $\psi_T$  in terms of  $\phi_T(k)$ :

$$\begin{aligned} \psi_T(v) &= \int_{-\infty}^\infty e^{ivk} \int_k^\infty e^{ak} e^{-rT} (e^s - e^k) q_T(s) ds dk \quad (52) \\ &= \int_{-\infty}^\infty e^{-rT} q_T(s) \int_{-\infty}^s (e^{s+ak} - e^{k+ak}) e^{ivk} dk ds \\ &= \int_{-\infty}^\infty e^{-rT} q_T(s) \left( \frac{e^{(a+1+iv)s}}{a+iv} - \frac{e^{(a+1+iv)s}}{a+1+iv} \right) ds \\ &= e^{-rT} \int_{-\infty}^\infty q_T(s) \frac{e^{(a+1+iv)s}}{(a+1+iv)(a+iv)} ds \\ &= \frac{e^{-rT} \phi_T(v - (a+1)i)}{a^2 + a - v^2 + i(2a+1)v} \end{aligned}$$

Using the known expression for the time changed Meixner characteristic function in Eq. (45) in Eq. (52), we can compute the option prices by using Eq. (51).

### 3.3.2 Fast Fourier transformation FFT

Fast Fourier transformation is an algorithm that efficiently calculates the sum:

$$\omega(k) = \sum_{j=1}^N e^{-i2\pi(j-1)(k-1)/N} x(j), \quad (53)$$

where  $N$  is usually in a power of 2. FFT is commonly used as a discrete approximation technique for the Fourier transformation that significantly reduce the computational burden. By using FFT we can approximate Eq. (51) by:

$$C_T(k) \approx \frac{\exp(-ak)}{\pi} \sum_{j=1}^N e^{-iv_j k} \psi_T(v_j) \eta \quad (54)$$

Madan and Carr suggest in their paper [7] the following parameter values and conventions:

$$\begin{aligned} v_j &= \eta(j-1), & N &= 2^{12} = 4096, & \alpha &= N\eta = 600, \\ b &= \frac{N\lambda}{2}, & k_u &= -b + \frac{2b}{N}(u-1), & \lambda\eta &= \frac{2\pi}{N} \end{aligned}$$

where  $\alpha$  is the upper limit of the integration,  $k_u$  is a vector with  $N$  values of  $k$ , and  $b$  sets a bound on the log strike to range in between  $[-b, b]$ . With these notations, Eq. (54) can be rewritten as:

$$C_T(k) \approx \frac{\exp(-ak_u)}{\pi} \sum_{j=1}^N e^{-i\lambda\eta(j-1)(u-1)} e^{ibv_j} \psi_T(v_j) \eta \quad (55)$$

Here, we cannot combine a too fine integration grid with a wide enough region for strikes since if we choose a small  $\eta$  that gives us a fine integration grid we will not cover many strike prices instead. Carr and Madan suggest to use Simpson's weighting rule to obtain an accurate enough integration with large  $\eta$ . Then we rewrite our pricing approximation formula one last time to:

$$C_T(k) \approx \frac{\exp(-ak_u)}{\pi} \sum_{j=1}^N e^{-i2\pi(j-1)(u-1)/N} e^{ibv_j} \psi_T(v_j) \frac{\eta}{3} (3 + (-i)^j - \delta_{j-1}), \quad (56)$$

where  $\delta_n$  is the Kronecker delta function. This is the price formula we will be using when calibrating our model parameters.

### 3.3.3 Calibration Results

We use historical option prices to calibrate the model parameters. The European call options of the S&P-500 index used as calibration is listed in Appendix A. The market prices were chosen between April 2016 to June 2017 with strike prices between 1700 and 2300. The index close price were on January 20th 2016 1881.3. While the pricing problem is the problem related

to price options given the parameter values, the calibration problem is the opposite: given the market prices of the options which model parameter values fits the data best? Here we are going to use the least square method in order to calibrate our model parameters. The idea is very simple: From the observed market prices  $(C_i)_{i=1}^N$  at  $t = 0$  for different strikes and maturities we try to minimize the difference of the proposed risk-neutral model prices,  $C^\theta$  with model parameters,  $\theta$ . Thus we find the best parameter values by minimizing the sum of the quadratic difference between these values:

$$\theta^* = \arg \min \sum_{i=1}^N (C_i - C^\theta(T_i, K_i))^2 \quad (57)$$

We are going to use a variation of this statistic as a measure of fit, called the Root Mean Square Error, RMSE:

$$\text{RMSE} = \sqrt{\sum_{i=1}^N \frac{(C_i - C^\theta(T_i, K_i))^2}{N}}$$

In the following tables the calibrated model parameters are shown together with the corresponding value of RMSE. We decided to calibrate both the model without a stochastic time change and with the integrated CIR-process to see the difference.

| Model       | Parameters |         |          |           |          |        |
|-------------|------------|---------|----------|-----------|----------|--------|
| Meixner     | $\alpha$   | $\beta$ | $\delta$ |           |          |        |
|             | 0.1843     | -1.1177 | 1.0707   |           |          |        |
| Meixner-CIR | $\alpha$   | $\beta$ | $\delta$ | $\lambda$ | $\kappa$ | $\eta$ |
|             | 0.1562     | -0.5358 | 3.3715   | 2.9849    | 0.2880   | 1.4860 |

Table 1: *Calibration results*

|             | Meixner | Meixner-CIR |
|-------------|---------|-------------|
| <b>RMSE</b> | 2.3237  | 0.5929      |

Table 2: *RMSE for the calibrations*

From the RMSE calculations we do notice that we get significantly better calibration results if we use an integrated CIR-process as a stochastic time change. In the following two figures we show the theoretical option prices from our calibrated model as well as the corresponding observed market prices:

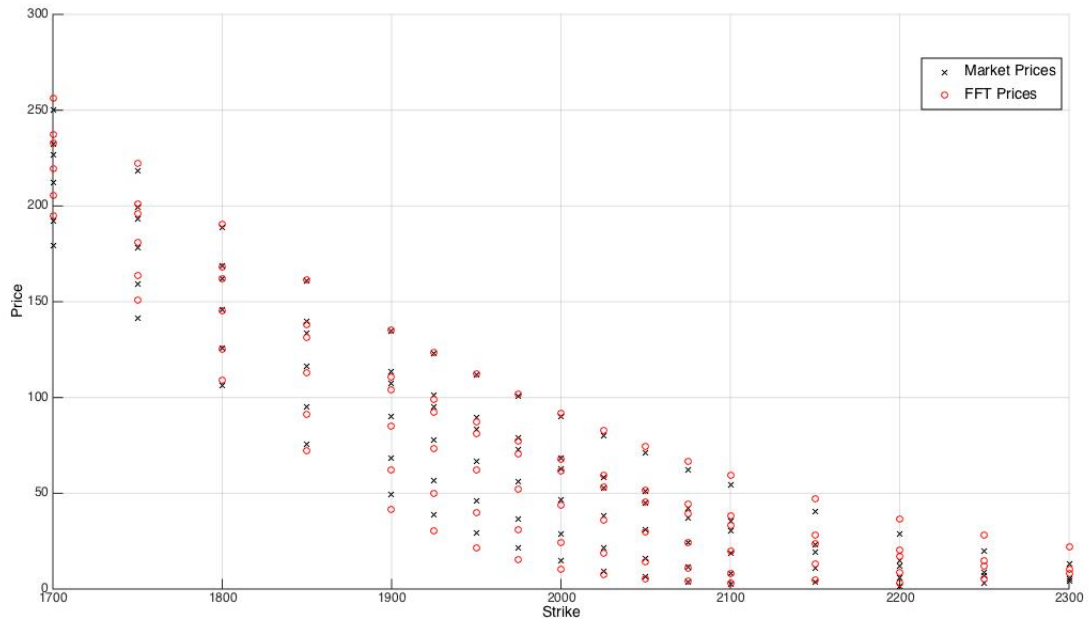


Figure 7: *Meixner calibration to S&P500 option prices*

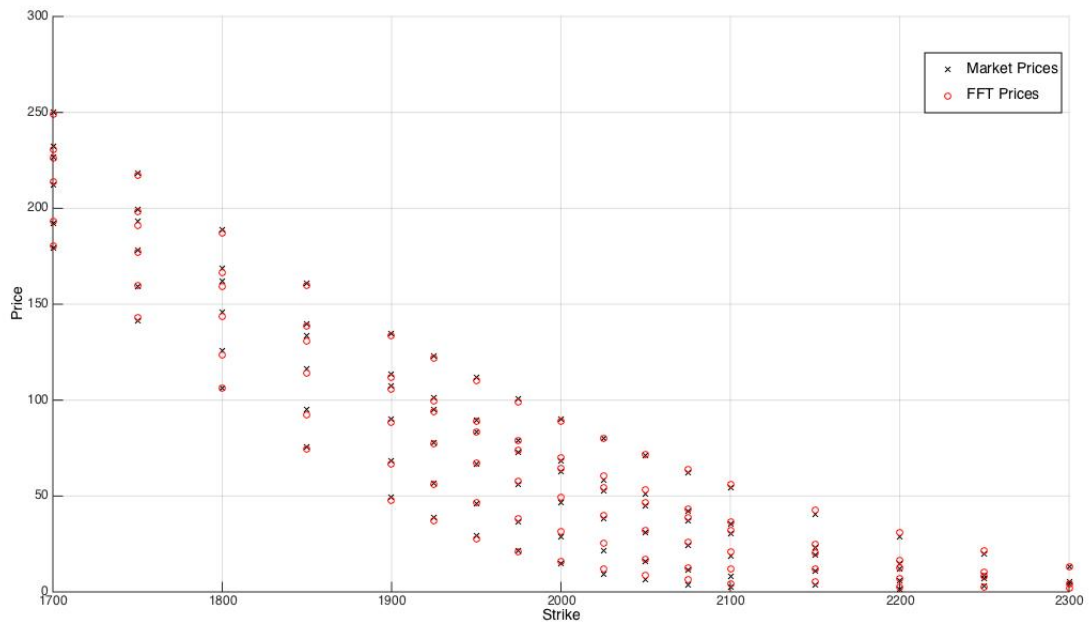


Figure 8: *Meixner-CIR calibration to S&P500 option prices*

### 3.4 Simulation Routine

There is no available closed form of the inverse cumulative density function of the multivariate Meixner distribution that we can use the inversion method to sample from. Hence in order to simulate from the multivariate Meixner process with integrated CIR-process we have to come up with another technique to simulate the Meixner process. The whole Monte Carlo simulation routine is as follows:

1. Simulate the rate of time change  $y_T$ ,  $0 \leq t \leq T$  from the CIR-process with either MC, QMC or RQMC simulations.
2. Calculate from (1) the time change  $Y_T = \int_0^T y_s ds$ ,  $0 \leq t \leq T$
3. Estimate the inverse multivariate Meixner distribution function,  $V^{-1}$ , with the parameters:  $\alpha$ ,  $\beta$  and  $\delta Y_T$  using Fourier transform techniques
4. Set  $X = V^{-1}(u)$ , where  $u$  is a uniform random vector in  $[0, 1]$  generated by MC, QMC or RQMC methods. The length of the vector,  $u$ , is equal to the number of underlying assets in the basket option. Repeat (1)-(4) until the desired amount of multivariate Meixner distributed random variables,  $X_T^{(N)}$ , is achieved.
5. The stock price at time  $T$  is then modeled as:  $S_T = S_0 \exp(X_{Y(T)})$
6. For each  $X^{(i)}$  calculate the payoff function  $g_i = G(S_T)$  where  $G$  is the payoff function described in equation (2).
7. Calculate the mean of the sample payoffs to get an estimate of the expected payoff:

$$\hat{g} = \frac{1}{N} \sum_{i=1}^N g_i$$

8. Discount the expected payoff at the risk-free interest rate to get an estimate of the value of the derivative:  $\exp(-rT)\hat{g}$



In the figure below we see a frequency plot from random samples of size 10000 from our simulation routine of the Meixner distribution. The dashed line represents the true Meixner density. The parameter values are the ones from the calibration results for the Meixner-CIR process:  $\alpha = 0.1562, \beta = -0.5358, \delta = 3.3715$ . As can be seen in the Figure 9 our routine fits the true Meixner density well.

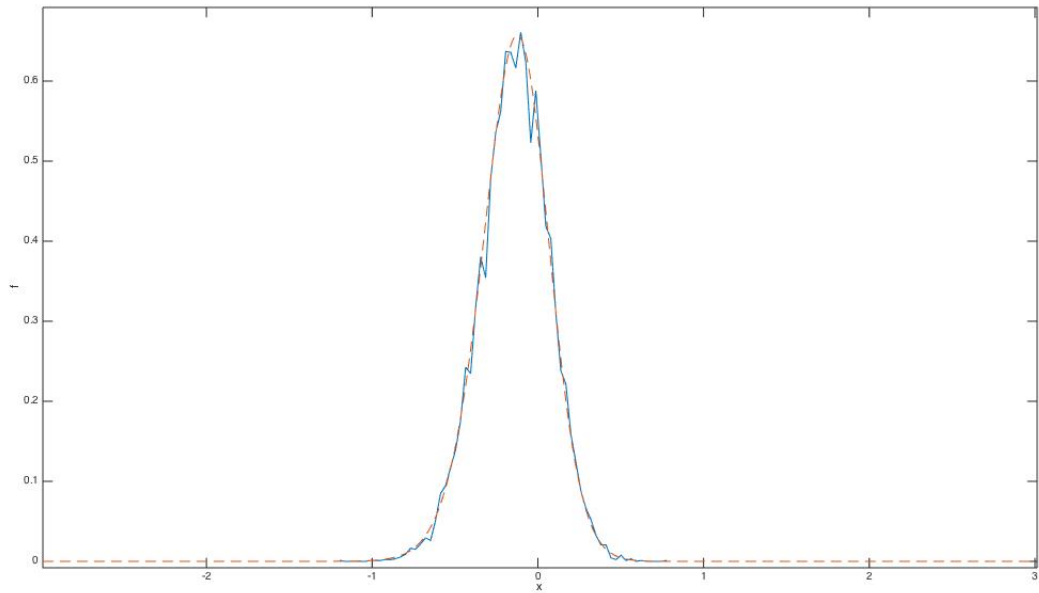


Figure 9: *Frequency plot for random samples from our Meixner distribution simulation routine*

## 4 Results

We apply the simulation algorithm with the different Monte Carlo-methods to price the basket options. The following data were used as input parameters for the numerical results: the number of assets in the basket is  $n = 4$ , the portfolio weights of each asset,  $w_i = 0.25$  for  $i = 1, \dots, n$ . The correlation coefficients  $\rho_{ij} = 0$  for  $i, j = 1, \dots, n$ . The initial asset prices  $S_i(0) = 1881.3$  for  $i = 1, \dots, n$ , the risk-free rate is set to 3% and the dividend yield is assumed to be 0%. The strike prices is set to  $K = 1700$  to  $K = 1900$  with increments of 100. We let maturity time be  $[1, 3]$ . Every estimation is done with 25000 simulations. In the simulations we use the calibrated parameter values from Table 1 in section 3.3.3.

Each of the five methods will be compared on both accuracy and speed. We will also simulate with and without stochastic time change and compare the differences in estimation and accuracy.

As a last result we will price vanilla options written on the S&P500-index and compare our theoretical prices with real market prices in order to get an understanding of how well our assumed underlying model fit the real world data as well as the efficiency of our simulation algorithms.

What we can see from the results is that depending on which model we use to model our assets, we get a different future belief in the market. Without an integrated CIR-process, the option prices tend to decrease with increasing maturity and increasing with maturity when using an integrated CIR-process.

### 4.1 Monte Carlo simulations of the Basket Option

In the first figures we see the basket option prices estimated with regular Monte Carlo simulation. In Figure 10 the three different basket options are estimated with the maturity time one year and with an integrated CIR-process. The blue line is the estimation with strike 1700, the red line is the estimation with strike 1800 and the green line is the estimation with strike 1900. In Figure 11 the maturity time is three years.

In Figure 12 and Figure 13 the basket options are estimated without an integrated CIR-process in the simulation routine. In Table 3 we see detailed data of the simulations. Assuming that the simulations with integrated CIR-process is the true value of the basket options we also compare how much closer to the real value the simulations are with a CIR-process as well as how much longer the simulation takes.

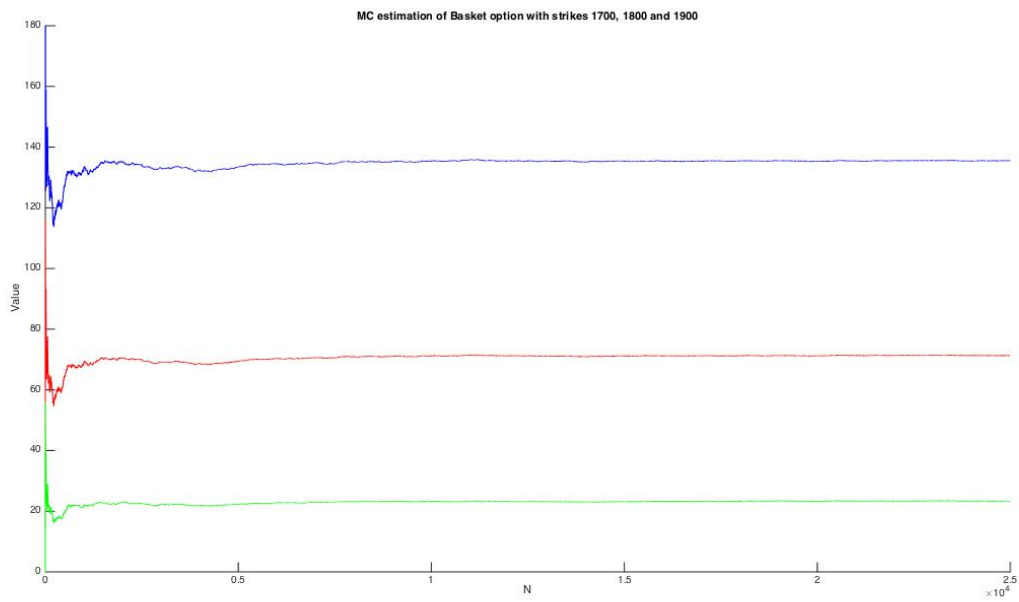


Figure 10: *Monte Carlo estimation of Basket options with strike 1700, 1800 and 1900. One year to maturity*

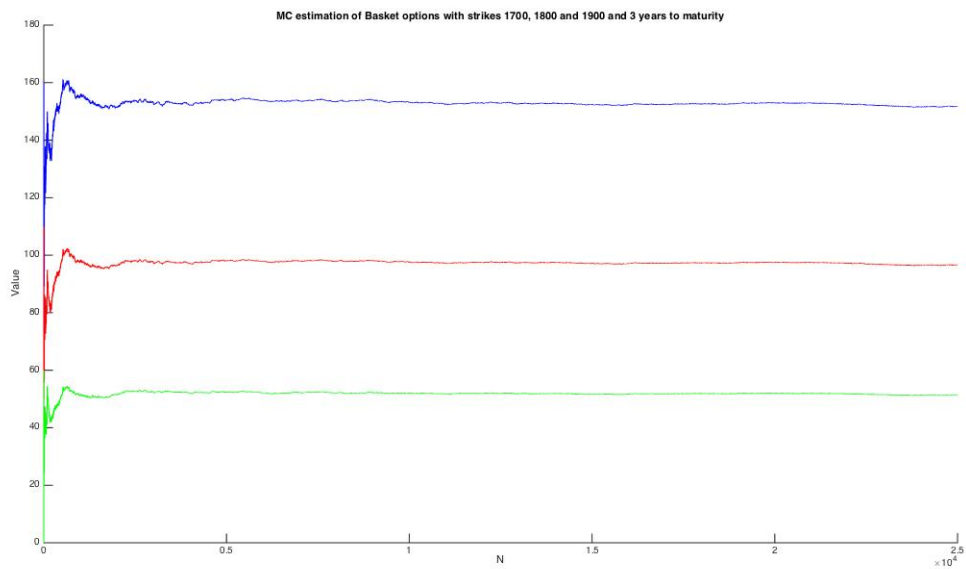


Figure 11: *Monte Carlo estimation of Basket options with strikes 1700, 1800 and 1900. Three years to maturity*

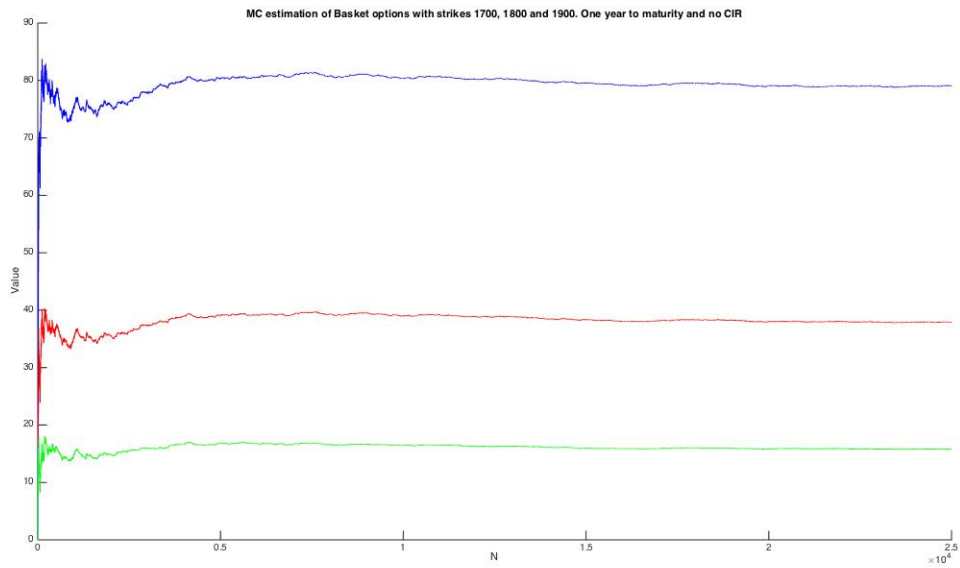


Figure 12: Monte Carlo estimation of Basket options with strikes 1700, 1800 and 1900. One year to maturity and no integrated CIR-process

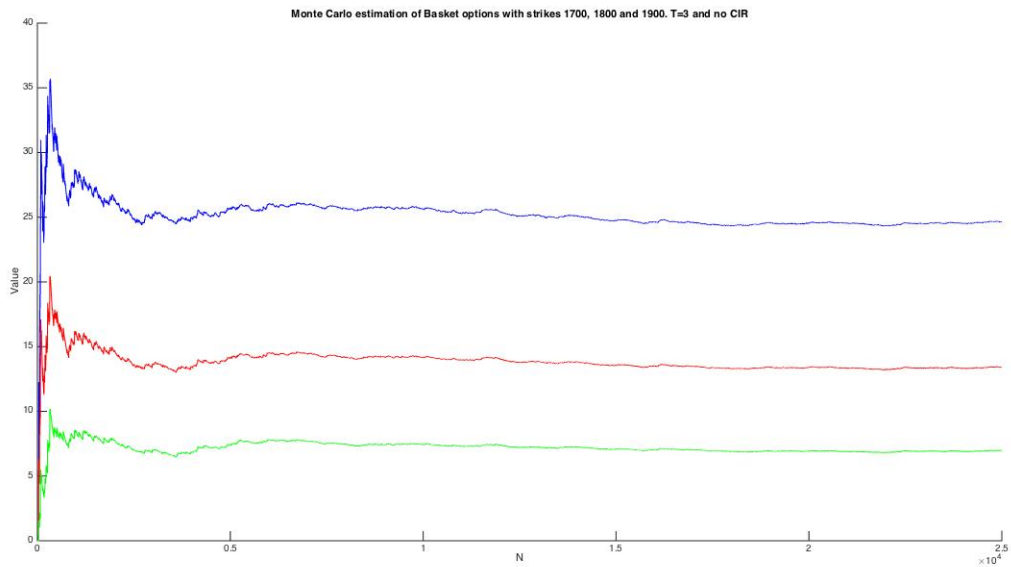


Figure 13: Monte Carlo estimation of Basket options with strikes 1700, 1800 and 1900. Three years to maturity and no integrated CIR-process

| <b>T</b>             | <b>K</b> | <b>MC with CIR (std)</b> | <b>MC no CIR (std)</b> |
|----------------------|----------|--------------------------|------------------------|
| 1                    | 1700     | 135.4839 (0.7488)        | 79.0191 (0.7267)       |
|                      | 1800     | 71.2894 (0.5219)         | 37.8910 (0.5168)       |
|                      | 1900     | 23.3244 (0.3000)         | 15.7767 (0.3322)       |
| <b>Comp.time (s)</b> |          | <b>654.78s</b>           | <b>503.60s</b>         |
| 3                    | 1700     | 151.6640 (1.0259)        | 24.6492 (0.9789)       |
|                      | 1800     | 96.5520 (0.7827)         | 13.4189 (0.7899)       |
|                      | 1900     | 51.3931 (0.5440)         | 6.9680 (0.5805)        |
| <b>Comp.time (s)</b> |          | <b>836.16s</b>           | <b>513.58s</b>         |

Table 3: *Results of the four different Monte Carlo simulations with the calibrated parameters from section 3.3.3*

In Table 4 we compare the extra computation time between using an integrated CIR-process and the accuracy of the estimation compared to not using an CIR-process. We assume the process with integrated CIR converges to the true value of the option.

| <b>T</b> | <b>K</b> | <b>Increased comp.time (%)</b> | <b>Increased accuracy (%)</b> |
|----------|----------|--------------------------------|-------------------------------|
| 1        | 1700     | 30.0 %                         | 41.7 %                        |
|          | 1800     | 30.0 %                         | 46.8 %                        |
|          | 1900     | 30.0 %                         | 32.4 %                        |
| 3        | 1700     | 62.8 %                         | 83.8 %                        |
|          | 1800     | 62.8 %                         | 86.1 %                        |
|          | 1900     | 62.8 %                         | 86.4 %                        |

Table 4: *Comparison between increased computation time and increased accuracy of using integrated CIR-process in the Monte Carlo simulations of the basket options when assuming the simulation with integrated CIR-process converges to the true option value*

## 4.2 Quasi-Monte Carlo simulations of the Basket Option

In the first subsection we give the results of the Sobol sequences and in the second subsection we give the results of the Halton sequences.

### 4.2.1 Sobol sets for estimating Basket options

In Figure 14 - Figure 17 the results of the simulations with Sobol sequences are presented for estimating the basket options. As in the Monte Carlo simulations, the blue line corresponds to strike 1700, the red line corresponds to strike 1800 and the green line corresponds to strike 1900.

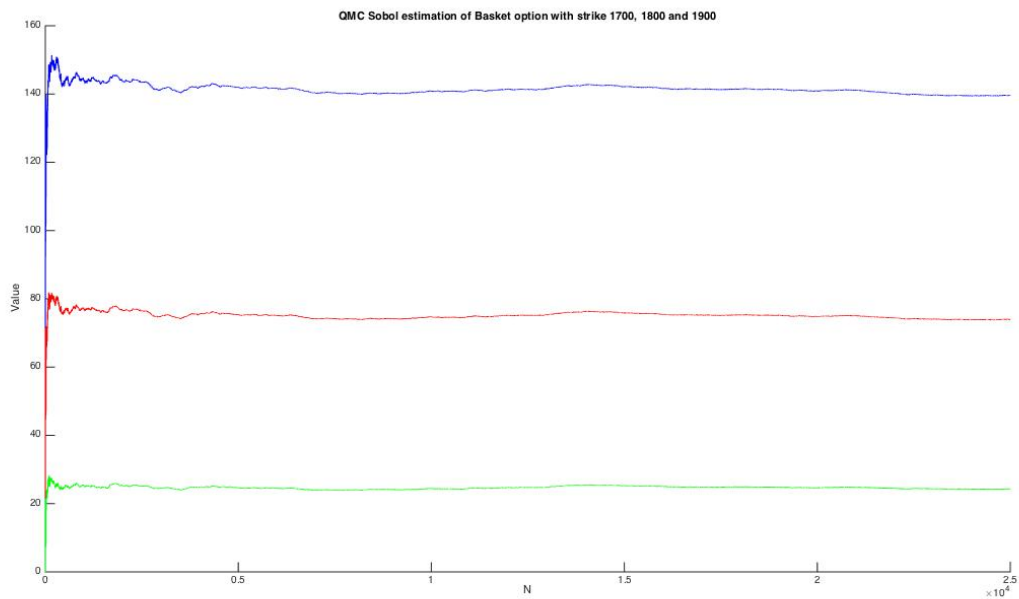


Figure 14: *Quasi-Monte Carlo with Sobol sequences estimation of Basket options with strike 1700, 1800 and 1900. One year to maturity*

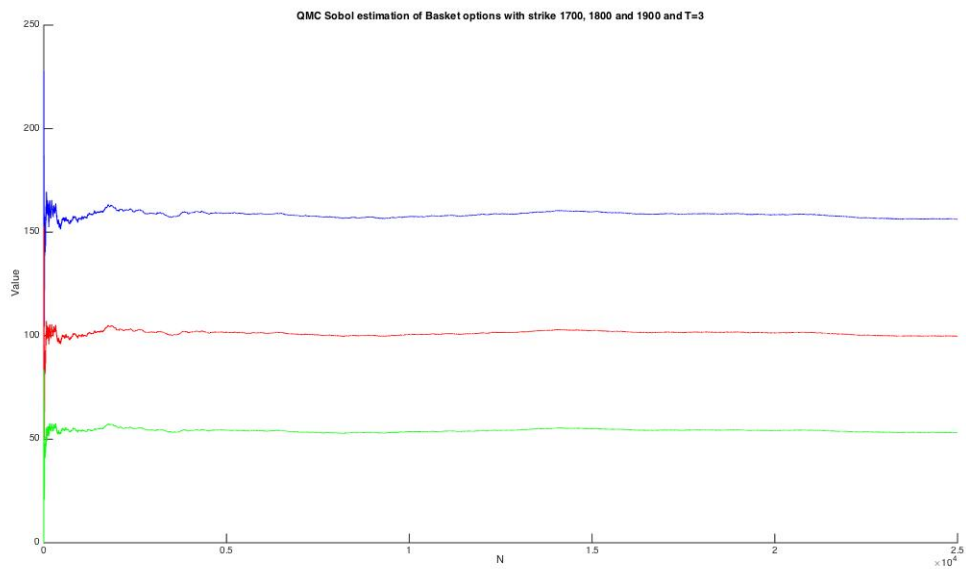


Figure 15: *Quasi-Monte Carlo with Sobol sequences estimation of Basket options with strike 1700, 1800 and 1900. Three years to maturity*

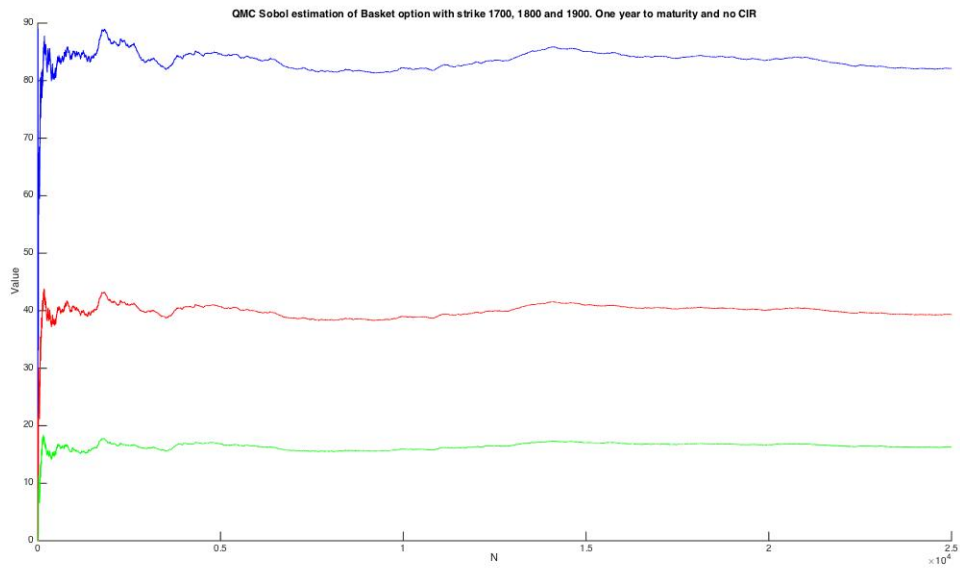


Figure 16: *Quasi-Monte Carlo with Sobol sequences estimation of Basket options with strike 1700, 1800 and 1900. One year to maturity and no integrated CIR-process*

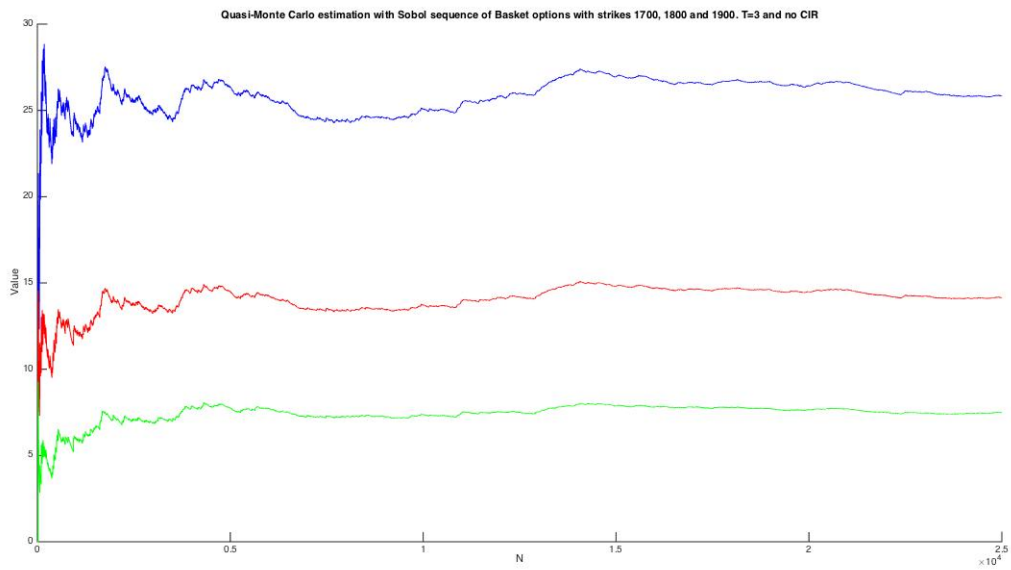


Figure 17: *Quasi-Monte Carlo with Sobol sequences estimation of Basket options with strike 1700, 1800 and 1900. Three years to maturity and no integrated CIR-process*

| <b>T</b>             | <b>K</b> | <b>QMC Sobol with CIR</b> | <b>QMC Sobol no CIR</b> |
|----------------------|----------|---------------------------|-------------------------|
| 1                    | 1700     | 139.5565                  | 82.0935                 |
|                      | 1800     | 73.9390                   | 39.3225                 |
|                      | 1900     | 24.2768                   | 16.2786                 |
| <b>Comp.time (s)</b> |          | <b>683.08s</b>            | <b>506.82s</b>          |
| 3                    | 1700     | 156.3356                  | 25.8455                 |
|                      | 1800     | 99.7679                   | 14.1523                 |
|                      | 1900     | 53.2036                   | 7.4797                  |
| <b>Comp.time (s)</b> |          | <b>738.25s</b>            | <b>535.01s</b>          |

Table 5: Results of the four different quasi-Monte Carlo simulations with a Sobol sequence and the calibrated parameters from section 3.3.3

In Figure 18 we have plotted both the Monte Carlo simulation and the quasi-Monte Carlo simulation with Sobol sequences in the same figure to easily compare the different simulations methods. Time to maturity is one year and includes an integrated CIR-process. The blue lines represent the quasi-Monte Carlo simulations and the red lines represent Monte Carlo simulation. We see that there are some discrepancy in the options estimations between the two methods.

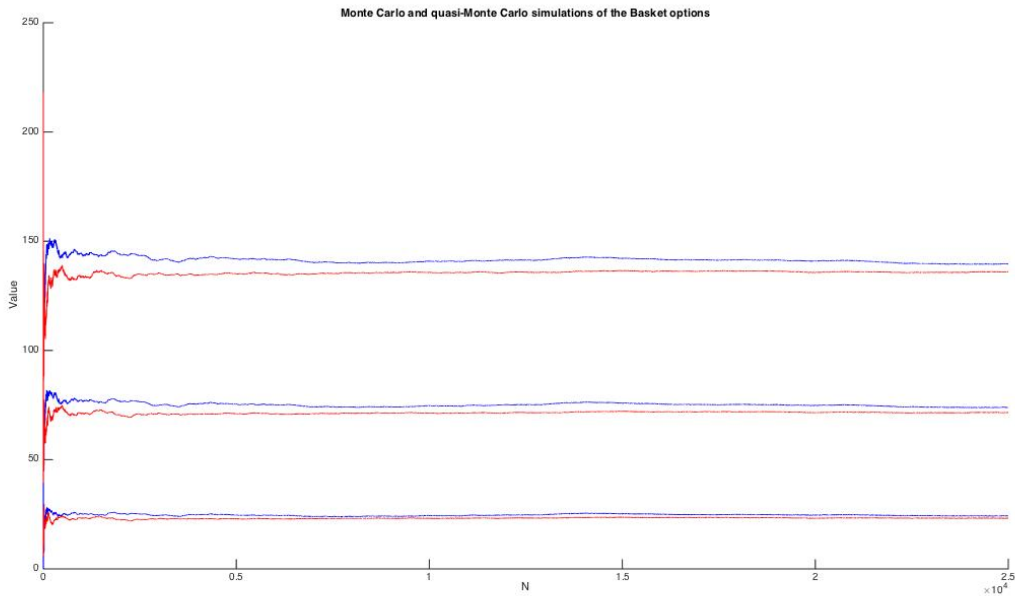


Figure 18: Monte Carlo and Quasi Monte Carlo with Sobol sequences estimation of Basket options with strike 1700, 1800 and 1900. One year to maturity



#### 4.2.2 Halton sets for estimating Basket options

In Figure 19 - Figure 22 the results of the simulations with Halton sequences are presented for estimating the basket options. As in the the other simulations, the blue line corresponds to strike 1700, the red line corresponds to strike 1800 and the green line corresponds to strike 1900. In Figure 19 and Figure 20 we do see that using Halton sequences in very high dimensional problems doesn't work very well. In the CIR-simulations we have problem of dimension 730 for the one year to maturity simulation and dimension 1111 in the three years to maturity simulation. Therefore we get poor estimations of the Basket options compared to the other estimation methods. However, using Halton sequences when estimating without a CIR-process we get comparable results as the other simulations and can be seen in Figure 21-22.

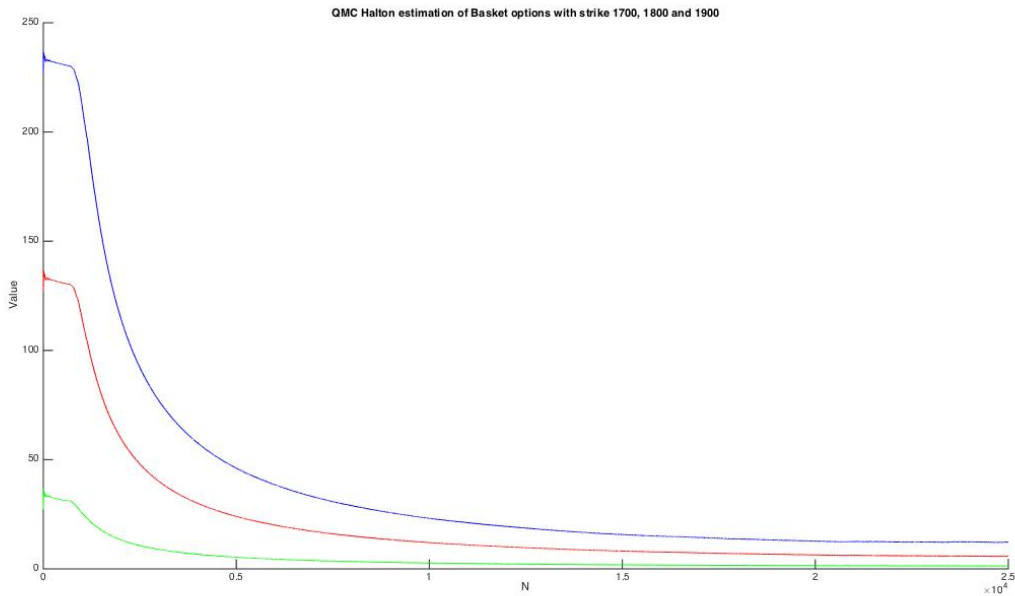


Figure 19: *Quasi-Monte Carlo with Halton sequences estimation of Basket options with strike 1700, 1800 and 1900. One year to maturity*

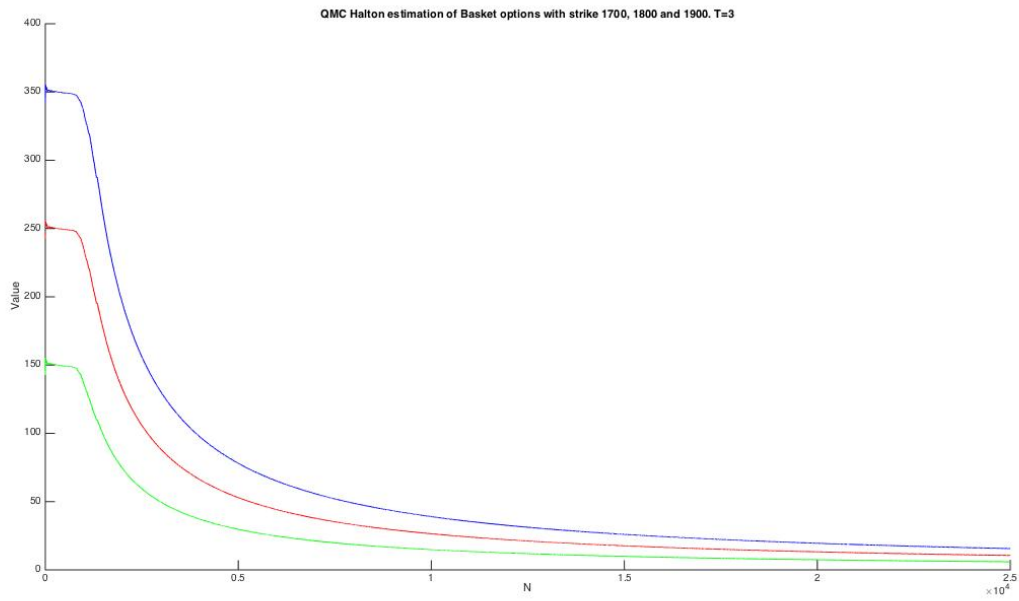


Figure 20: *Quasi-Monte Carlo with Halton sequences estimation of Basket options with strike 1700, 1800 and 1900. Three years to maturity*

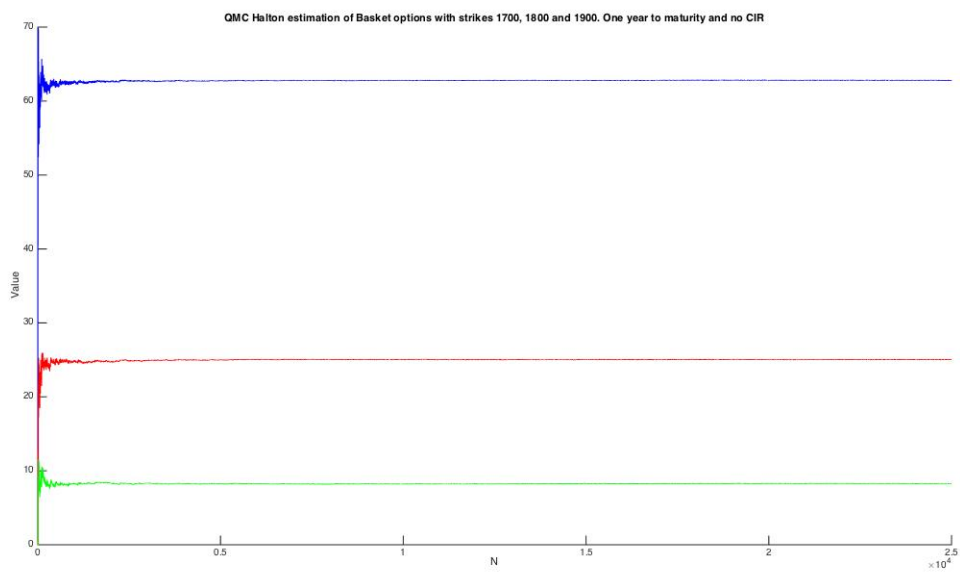


Figure 21: *Quasi-Monte Carlo with Halton sequences estimation of Basket options with strike 1700, 1800 and 1900. One year to maturity and no integrated CIR-process*

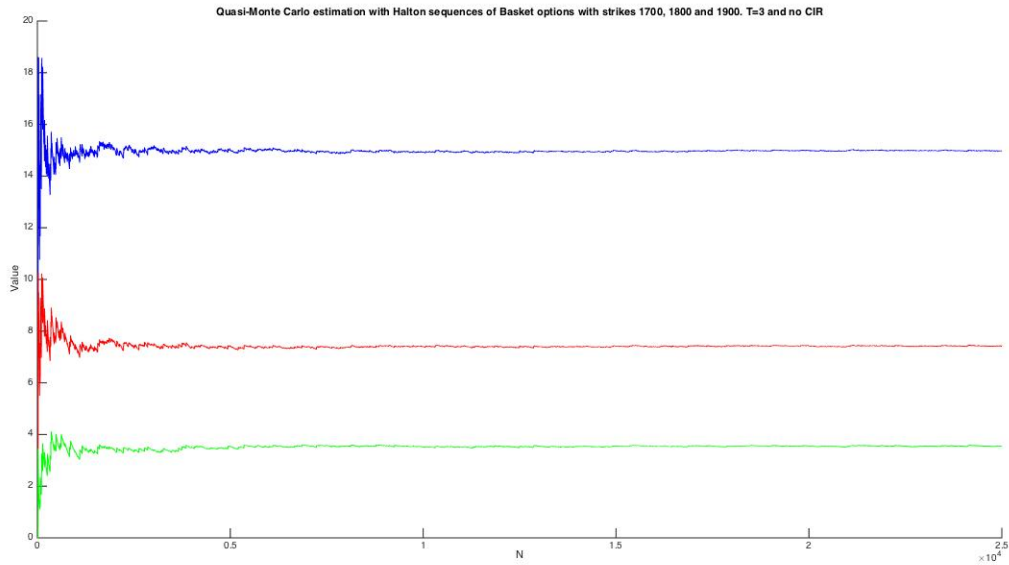


Figure 22: *Quasi-Monte Carlo with Halton sequences estimation of Basket options with strike 1700, 1800 and 1900. Three years to maturity and no integrated CIR-process*

| <b>T</b>             | <b>K</b> | <b>QMC Halton with CIR</b> | <b>QMC Halton no CIR</b> |
|----------------------|----------|----------------------------|--------------------------|
| 1                    | 1700     | 12.2429                    | 62.8002                  |
|                      | 1800     | 5.7182                     | 25.0498                  |
|                      | 1900     | 1.3224                     | 8.2626                   |
| <b>Comp.time (s)</b> |          | <b>799.71s</b>             | <b>513.15s</b>           |
| 3                    | 1700     | 15.6076                    | 14.9662                  |
|                      | 1800     | 10.5845                    | 7.4163                   |
|                      | 1900     | 5.9430                     | 3.5426                   |
| <b>Comp.time (s)</b> |          | <b>1170.53s</b>            | <b>512.71s</b>           |

Table 6: *Results of the four different quasi-Monte Carlo simulations with a Halton sequence and the calibrated parameters from section 3.3.3*

### 4.3 Randomized quasi-Monte Carlo simulations of the Basket Option

In the first subsection we give the results from the randomized quasi-Monte Carlo method with Sobol sequences. In the second subsection we give the results from the randomized quasi-Monte Carlo simulations with Halton sequences. Every simulation is done with  $N = 158$  and  $I = 158$  this gives us a total of 24964 simulations. In this thesis we will not consider adjusting  $N$  and  $I$  in order to achieve better results. We finish the section by showing a table with all five different simulation methods' numerical values.

#### 4.3.1 Randomized quasi-Monte Carlo Simulation with Sobol sequences

In Figure 23 - Figure 26 the results of the simulations with Randomized quasi-Monte Carlo simulations with Sobol sequences are presented for estimating the basket options. As in the other simulations, the blue line corresponds to strike 1700, the red line corresponds to strike 1800 and the green line corresponds to strike 1900.

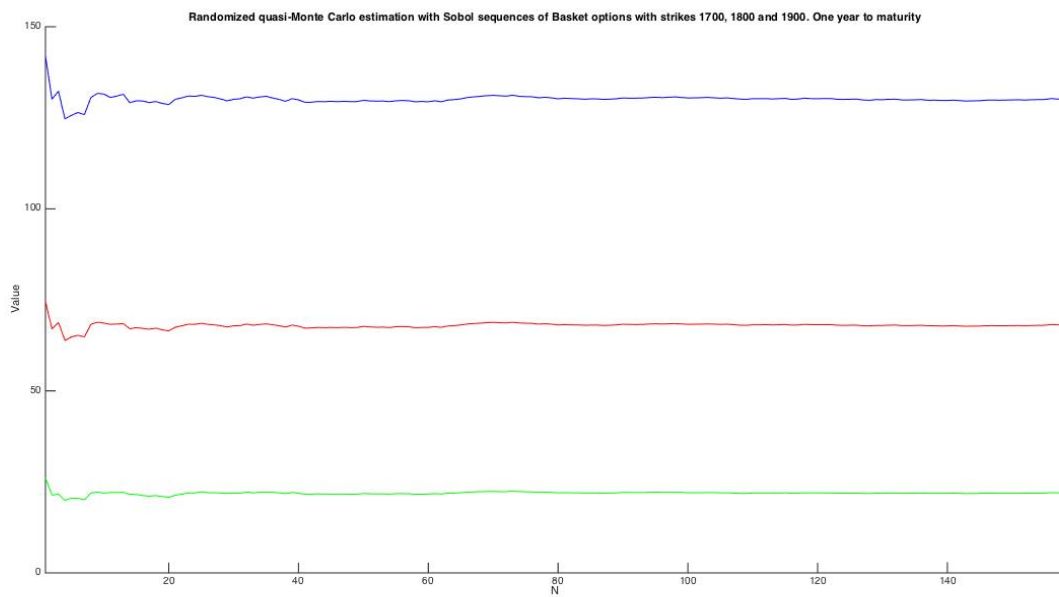


Figure 23: *Randomized quasi-Monte Carlo with Sobol sequences estimation of Basket options with strike 1700, 1800 and 1900. One year to maturity*

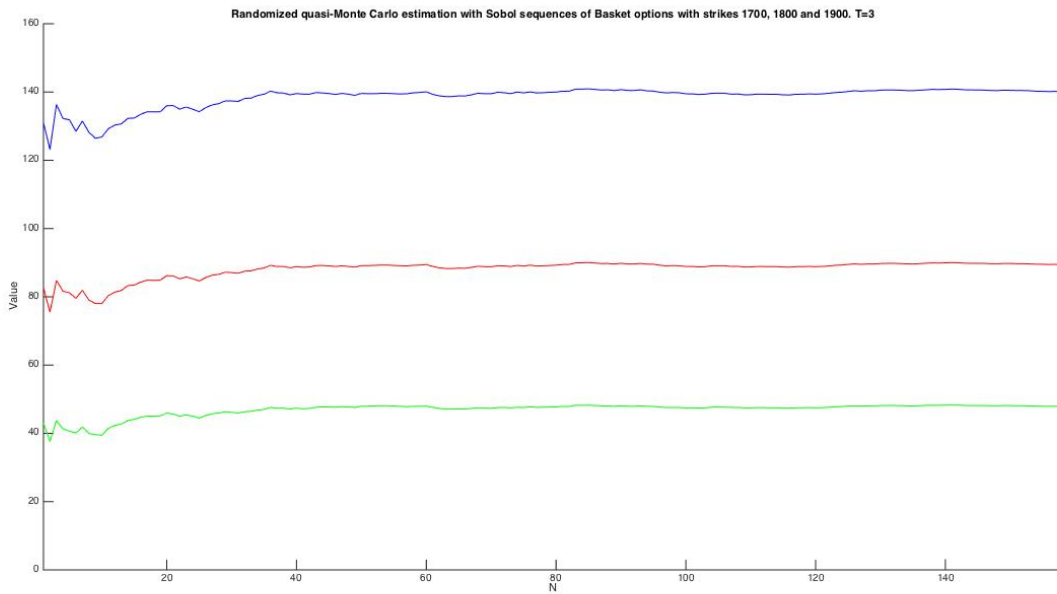


Figure 24: *Randomized quasi-Monte Carlo with Sobol sequences estimation of Basket options with strike 1700, 1800 and 1900. Three years to maturity*

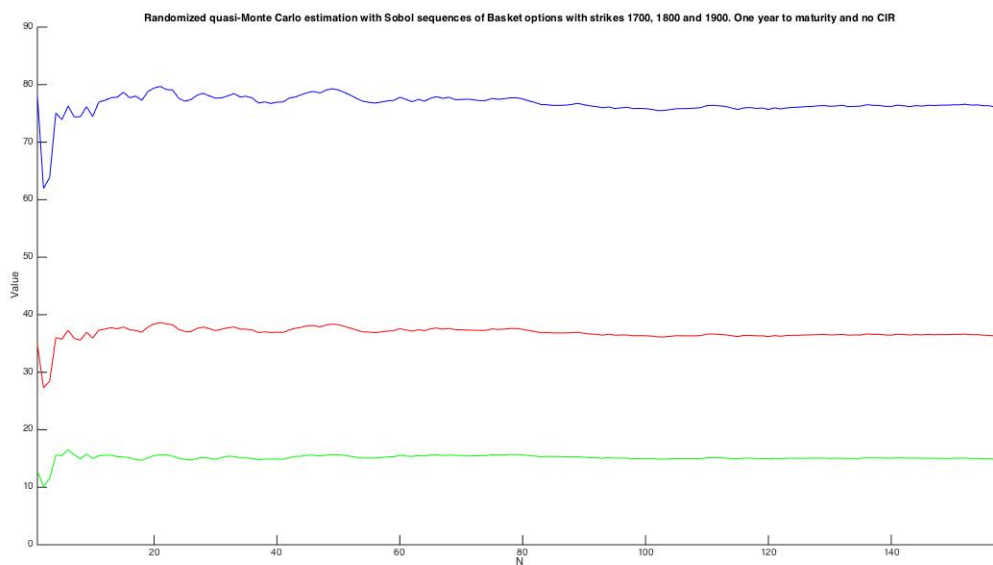


Figure 25: *Randomized quasi-Monte Carlo with Sobol sequences estimation of Basket options with strike 1700, 1800 and 1900. One year to maturity and no integrated CIR-process*

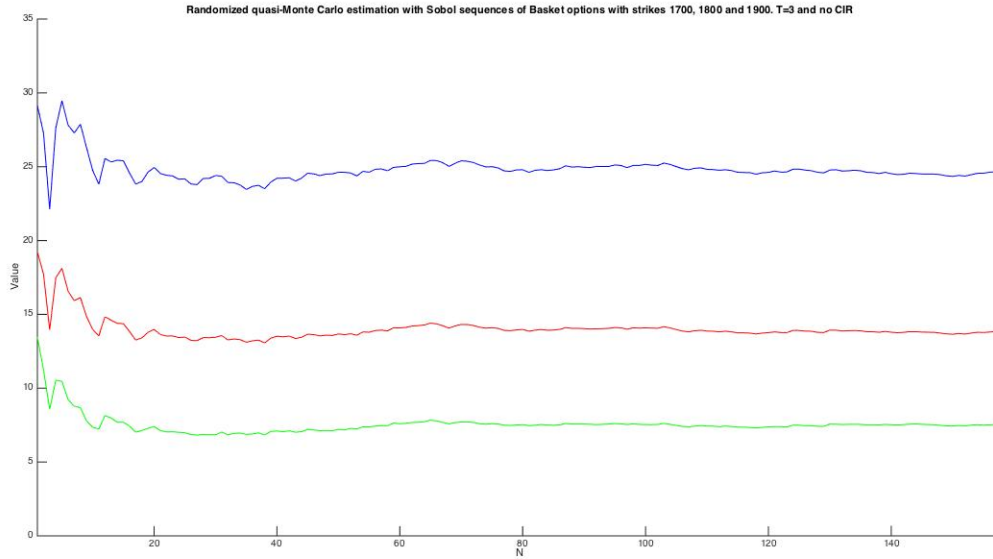


Figure 26: *Randomized quasi-Monte Carlo with Sobol sequences estimation of Basket options with strike 1700, 1800 and 1900. Three years to maturity and no integrated CIR-process*

| <b>T</b>          | <b>K</b> | <b>RQMC Sobol with CIR (std)</b> | <b>RQMC Sobol no CIR (std)</b> |
|-------------------|----------|----------------------------------|--------------------------------|
| 1                 | 1700     | 130.1303 (0.7712)                | 76.3333 (0.6988)               |
|                   | 1800     | 68.1333 (0.5134)                 | 36.4356 (0.5017)               |
|                   | 1900     | 22.0055 (0.3360)                 | 14.9842 (0.2519)               |
| <b>C.time (s)</b> |          | <b>617.40s</b>                   | <b>474.49s</b>                 |
| 3                 | 1700     | 140.0488 (0.8188)                | 24.5826 (0.7883)               |
|                   | 1800     | 89.3890 (0.7023)                 | 13.7676 (0.5385)               |
|                   | 1900     | 47.8425 (0.5122)                 | 7.4976 (0.3815)                |
| <b>C.time (s)</b> |          | <b>668.15s</b>                   | <b>508.80s</b>                 |

Table 7: *Results of the four different randomized quasi-Monte Carlo simulations with a Sobol sequence and the calibrated parameters from section 3.3.3*

### 4.3.2 Randomized quasi-Monte Carlo Simulation with Halton sequences

In Figure 27 - Figure 30 the results of the simulations with Randomized quasi-Monte Carlo simulations with Halton sequences are presented for estimating the basket options. As in all the other simulations, the blue line corresponds to strike 1700, the red line corresponds to strike 1800 and the green line corresponds to strike 1900.

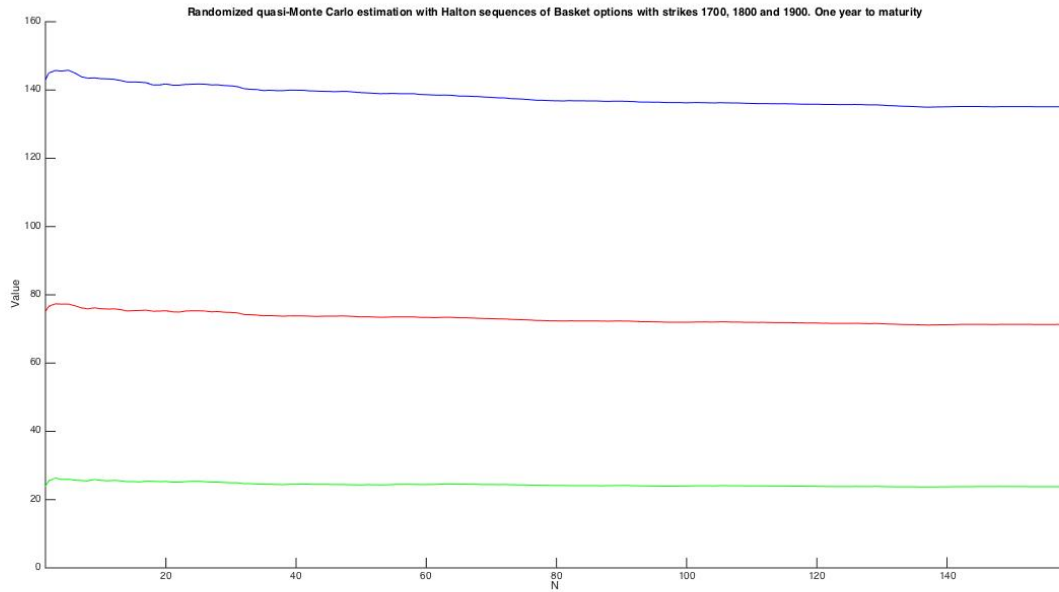


Figure 27: *Randomized quasi-Monte Carlo with Halton sequences estimation of Basket options with strike 1700, 1800 and 1900. One year to maturity*

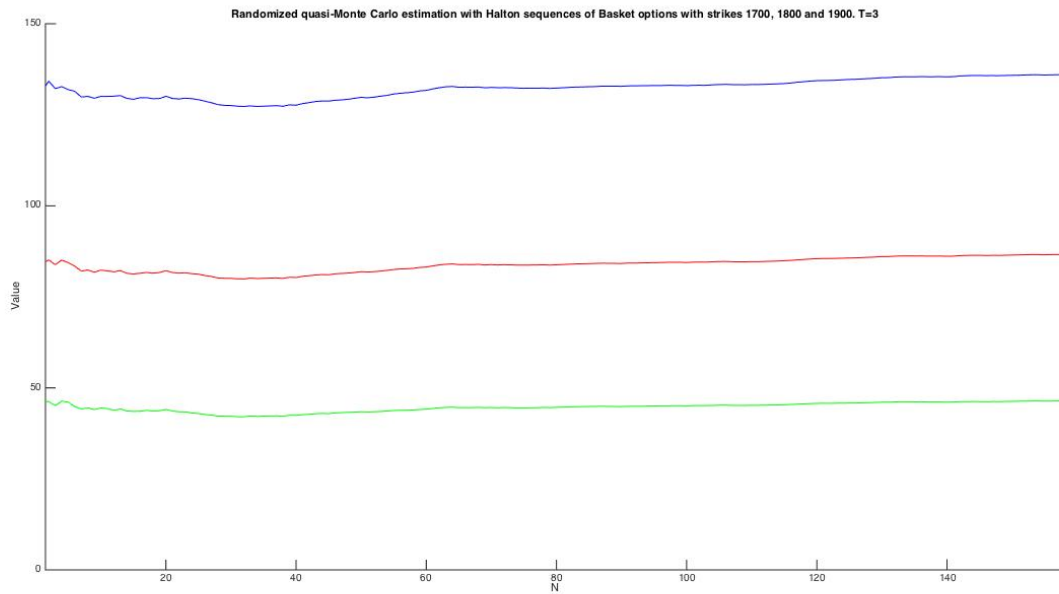


Figure 28: *Randomized quasi-Monte Carlo with Halton sequences estimation of Basket options with strike 1700, 1800 and 1900. Three years to maturity*

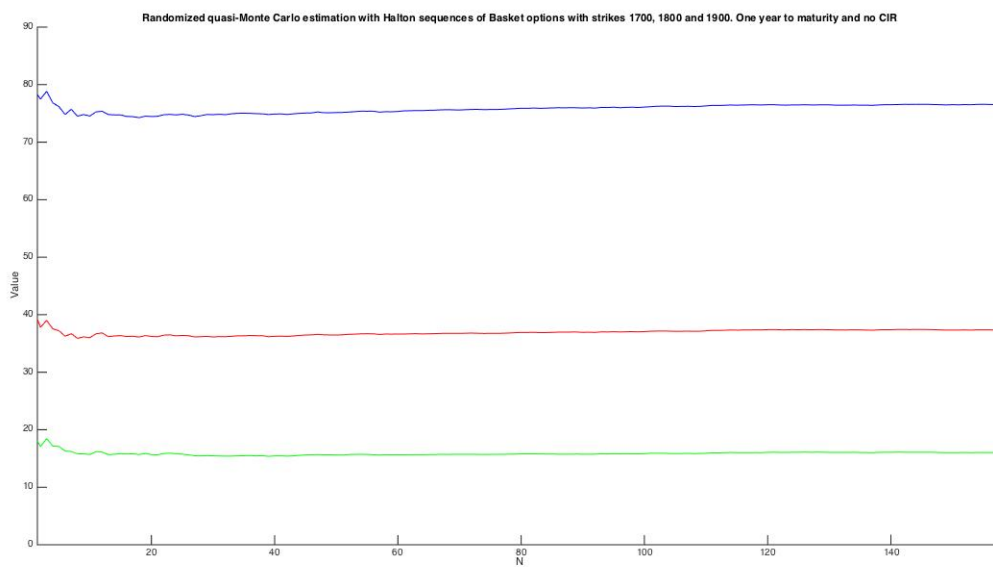


Figure 29: *Randomized quasi-Monte Carlo with Halton sequences estimation of Basket options with strike 1700, 1800 and 1900. One year to maturity and no integrated CIR-process*



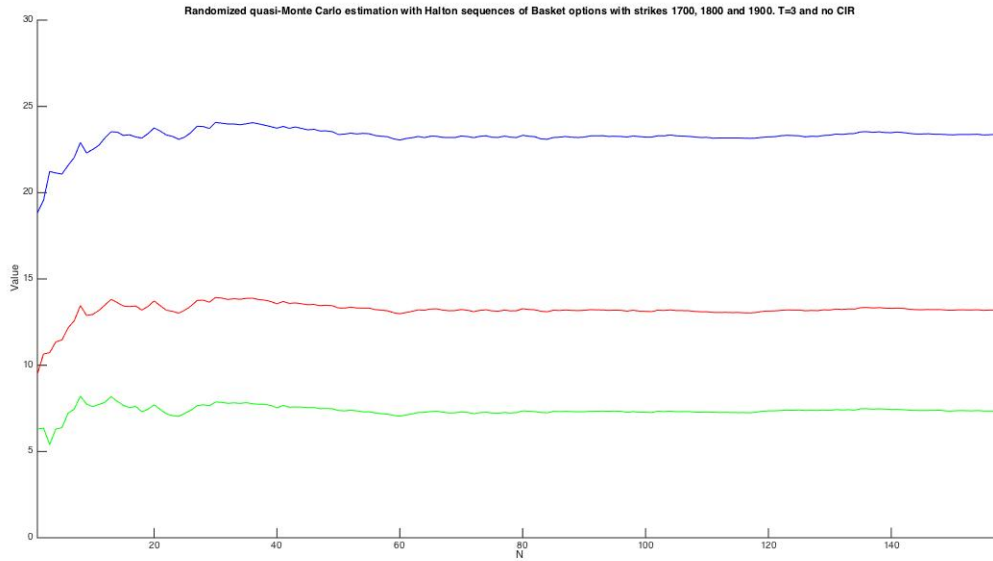


Figure 30: *Randomized quasi-Monte Carlo with Halton sequences estimation of Basket options with strike 1700, 1800 and 1900. Three years to maturity and no integrated CIR-process*

| <b>T</b>          | <b>K</b> | <b>RQMC Halton with CIR (std)</b> | <b>RQMC Halton no CIR (std)</b> |
|-------------------|----------|-----------------------------------|---------------------------------|
| 1                 | 1700     | 135.1000 (0.5230)                 | 76.5373 (0.3628)                |
|                   | 1800     | 71.2993 (0.3811)                  | 37.3290 (0.2924)                |
|                   | 1900     | 23.7775 (0.2352)                  | 16.0242 (0.2292)                |
| <b>C.time (s)</b> |          | <b>609.39s</b>                    | <b>474.20s</b>                  |
| 3                 | 1700     | 136.0302 (0.7881)                 | 23.3948 (0.3610)                |
|                   | 1800     | 86.6339 (0.6146)                  | 13.1931 (0.3178)                |
|                   | 1900     | 46.3919 (0.4316)                  | 7.3306 (0.2712)                 |
| <b>C.time (s)</b> |          | <b>662.74s</b>                    | <b>517.12s</b>                  |

Table 8: *Results of the four different randomized quasi-Monte Carlo simulations with a Halton sequences and the calibrated parameters from section 3.3.3*

Finally we summarize our simulations in Table 9 and Table 10 with the numerical values of the different simulations. Both with the market model including an integrated CIR-process as well as the model without a CIR-process.

| <b>T</b> | <b>K</b>    | <b>MC</b>     | <b>QMCS</b> | <b>QMCH</b> | <b>RQMCS</b>  | <b>RQMCH</b>  |
|----------|-------------|---------------|-------------|-------------|---------------|---------------|
| <b>1</b> | <b>1700</b> | 135.48 (0.75) | 139.56      | 12.24       | 130.13 (0.77) | 135.10 (0.52) |
|          | <b>1800</b> | 71.29 (0.52)  | 73.94       | 5.72        | 68.13 (0.51)  | 71.30 (0.38)  |
|          | <b>1900</b> | 23.32 (0.30)  | 24.28       | 1.32        | 22.00 (0.34)  | 23.78 (0.24)  |
| <b>3</b> | <b>1700</b> | 151.66 (1.03) | 156.34      | 15.61       | 140.05 (0.82) | 136.03 (0.79) |
|          | <b>1800</b> | 96.55 (0.78)  | 99.77       | 10.58       | 89.39 (0.70)  | 86.63 (0.61)  |
|          | <b>1900</b> | 51.39 (0.54)  | 53.20       | 5.94        | 47.84 (0.51)  | 46.39 (0.43)  |

Table 9: *Comparison of the numerical values of the different simulation techniques with an integrated CIR-process. Standard deviation of the simulations are presented in the parentheses*

| <b>T</b> | <b>K</b>    | <b>MC</b>    | <b>QMCS</b> | <b>QMCH</b> | <b>RQMCS</b> | <b>RQMCH</b> |
|----------|-------------|--------------|-------------|-------------|--------------|--------------|
| <b>1</b> | <b>1700</b> | 79.02 (0.73) | 82.09       | 62.80       | 76.33 (0.70) | 76.54 (0.36) |
|          | <b>1800</b> | 37.89 (0.52) | 39.32       | 25.05       | 36.44 (0.50) | 37.33 (0.29) |
|          | <b>1900</b> | 15.78 (0.33) | 16.28       | 8.26        | 14.98 (0.25) | 16.02 (0.23) |
| <b>3</b> | <b>1700</b> | 24.65 (0.98) | 25.86       | 14.97       | 24.58 (0.79) | 23.39 (0.36) |
|          | <b>1800</b> | 13.42 (0.79) | 14.15       | 7.42        | 13.77 (0.54) | 13.19 (0.32) |
|          | <b>1900</b> | 6.97 (0.58)  | 7.48        | 3.54        | 7.50 (0.38)  | 7.33 (0.27)  |

Table 10: *Comparison of the numerical values of the different simulation techniques without an integrated CIR-process. Standard deviation of the simulations are presented in the parentheses*

#### 4.4 Model fit to real values

As a last result, we are going to check whether the accuracy of our described simulation approach is good compared to real market data. We do this by pricing European vanilla call options written on the S&P500-index with maturity date 16th of June 2017, and compare the simulated prices with the corresponding real world market prices fetched from Nasdaq on the 20th of January 2016. This gives us  $T = 1.402$  years. Number of simulations are 25000. By doing this comparison we have both evaluated the different simulation methods to each other as well as how well the assumed underlying model fits the real world data. The closed index price is  $S_0 = 1881.30$ . The results were as follows:

| Strike | MC            | QMCH   | QMCS   | RQMCH         | RQMCS         | Mean of Bid & Ask |
|--------|---------------|--------|--------|---------------|---------------|-------------------|
| 1700   | 211.24 (1.53) | 143.87 | 213.69 | 213.72 (0.69) | 211.06 (0.65) | 250.20            |
| 1750   | 181.27 (1.43) | 124.65 | 183.40 | 183.43 (0.61) | 181.29 (0.56) | 218.55            |
| 1800   | 152.93 (1.33) | 107.29 | 154.71 | 154.68 (0.54) | 153.10 (0.49) | 188.75            |
| 1850   | 126.46 (1.23) | 91.73  | 127.86 | 127.78 (0.49) | 126.72 (0.43) | 160.80            |
| 1900   | 102.19 (1.14) | 77.79  | 103.20 | 103.00 (0.45) | 102.42(0.39)  | 134.85            |
| 1950   | 80.50 (1.04)  | 65.54  | 81.00  | 80.75 (0.43)  | 80.62 (0.38)  | 111.60            |
| 2000   | 61.79 (0.95)  | 55.86  | 61.95  | 61.58 (0.42)  | 61.81 (0.38)  | 90.10             |
| 2050   | 46.54 (0.86)  | 47.80  | 46.72  | 46.15 (0.39)  | 46.52 (0.36)  | 71.05             |
| 2100   | 35.24 (0.78)  | 40.93  | 35.69  | 34.82 (0.37)  | 35.16 (0.34)  | 54.50             |
| 2150   | 26.99 (0.70)  | 35.09  | 27.55  | 26.63 (0.36)  | 26.94 (0.33)  | 40.15             |
| 2200   | 20.84 (0.64)  | 30.13  | 21.41  | 20.60 (0.34)  | 20.89 (0.31)  | 28.95             |

Table 11: *Theoretical prices with estimated standard deviation and market prices for European Call Options*

The prices are estimated using the same parameters estimated in section 3.3.3 and with an integrated CIR-process. Once again we notice that estimating with Halton sequences in high dimensional problems doesn't yield as satisfactory results as the other methods.

## 5 Conclusions

In this master thesis we investigated the pricing of basket options using different kinds of Monte Carlo methods and a time changed Meixner Lévy process as assumed underlying process. We began with pricing European options using fast Fourier transformation for Lévy processes since it is easy to find the characteristic function for most of the Lévy processes. The FFT-pricing was used for calibration of our model parameters that were being used in the Monte Carlo simulations. We have analyzed and compared the efficiency of standard Monte Carlo methods, quasi-Monte Carlo methods and randomized quasi-Monte Carlo methods.

The theoretical properties of the Meixner distribution, with heavier tails than the normal distribution and infinite divisibility, make it potentially very effective in modeling financial derivatives. However, the usefulness of a certain distribution depends also on the availability of algorithms to simulate from it, and to estimate its parameters. In this thesis we have come up with a simulation algorithm that let us use the inversion method to draw Meixner distributed variables and hence enable us to use randomized quasi-Monte Carlo methods to evaluate European basket options.

We do see that using an integrated CIR-process in the financial model has a big impact on pricing the derivatives and should be used in order to capture the volatility smile effect that market data shows. Depending on whether we include a CIR-process or not we got a different belief in the future of the underlying assets, which indicates that model choice has a huge impact on modeling the option prices. Using an integrated CIR-process to represent a stochastic time change minimizes the discrepancy between market prices and theoretical computed prices. However, using an integrated CIR-process with the inversion method also significantly increased the computation time. It all comes down to a trade off between increased computation time and increased accuracy (compared to market data) depending on preferences of the person simulating. The results of our simulations compared to real market data were okay but not extraordinary even when using an integrated CIR-process.

Theoretically, using randomized quasi-Monte Carlo methods can potentially increase the estimation accuracy significantly. We do see in our simulations that especially in the cases where we have a longer time to maturity, we get lower standard deviation of our simulations with the same cost of computation time. As well as in the vanilla option estimation we got significantly lower standard deviation with the RQMC methods. There exist no superior method for pricing basket options and analytical approximations do contain rather large approximation errors in some cases. We showed that by using randomized quasi-Monte Carlo methods with Sobol or Halton sequences we were able to increase the accuracy but the Monte Carlo methods are still very time consuming compared to other pricing methods. Until fast and accurate

analytical approximations of the basket options exist we do see that the using of randomized quasi-Monte Carlo can fulfill a good purpose of speeding up the estimation time and give accurate results of the basket option prices.

In the theory of quasi-Monte Carlo methods one of the biggest issue is the sensitivity of the dimension of the problem. In this thesis we have shown that using Halton sequences in very high-dimensional problems indeed yield bad results. But using Sobol sequences don't show the same behaviour and perform inline with the other Monte Carlo methods even in very high dimensions. However, using randomized quasi-Monte Carlo with Halton sequences yields higher accuracy in the simulations compared to using Sobol sequences.

One obvious limitation of the results in this thesis is that we don't compare other simulation techniques with the randomized quasi-Monte Carlo methods. Using randomized quasi-Monte Carlo methods limits us to the inversion method but there are also other techniques such as rejection sampling we don't even consider who could potentially be even more efficient.

In this thesis we have not investigated the performance of the randomized quasi-Monte Carlo methods by altering  $N$  and  $I$  which could have been an interesting aspect to look into. We leave this issue to someone else to investigate. Another interesting area we haven't consider in this thesis is to compare other Lévy processes with randomized quasi-Monte Carlo methods or to use other types of time changes than the CIR-process. For example, Belomestny does in his article [2] assume the time change process is unknown and estimate the characteristics of different Lévy processes from market data, which could be an interesting aspect of this master thesis' topic.

## References

- [1] Ané, T. and Geman, H. (2000) Order flow, transaction clock, and normality of asset returns'. *The Journal of Finance* **55** 2259-2284
- [2] Belomestny, D. (2011) Statistical inference for time-changed Lévy processes via composite characteristic function estimation. *The Annals of Statistics* **39** 2205-2242
- [3] Bertoin, J. (1998) Lévy Processes. *American Mathematical Society* **35** 343-346
- [4] Broadie, M. and Detemple, J.B. (2004) Option Pricing: Valuation Models and Applications. *Management Science* **50** 1145-1177
- [5] Caffisch, R.E. (1998) Monte Carlo and quasi-Monte Carlo methods. *Acta Numerica* 1-49
- [6] Carr, P., Geman, H., Madan, D. and Yor, M. (2003) Stochastic Volatility for Lévy Processes. *Mathematical Finance* **13** 345-382
- [7] Carr, P. and Madan, D.H. (1998). Option Valuation using fast Fourier transformation. *Journal of Computational Finance* **2** 61-73
- [8] Dalal, I.L., Stefan, D. and Harwayne-Gidansky, J. (2008) Low Discrepancy Sequences for Monte Carlo Simulations on Reconfigurable Platforms *Application Specific Systems, Architectures and Processors Conference* 108-113
- [9] Davis, P.J. and Rabinowitz, P. (1984) Methods of numerical integration. Brown University. Academic Press
- [10] Delbaen, F. and Schachermayer, W. (1994) A general version of the fundamental theorem of asset pricing. *Mathematische Annalen* **300** 463-520
- [11] Dybvig, P. and Ross, S.A. (1982) Portfolio Efficient Sets. *Econometrica, Econometric Society* **50** 1525-1546
- [12] Fox, B.L. (1999) Strategies for quasi-Monte Carlo. *Springer Science*, New York
- [13] Frittelli, M. (2000) Introduction to a Theory of Value Coherent with the No-Arbitrage Principle. *Finance and Stochastics* **4** 275-297
- [14] Gerber, H. and Shiu, E. (1994) Option pricing by Esscher transforms. *Transactions of Society of Actuaries* **46**
- [15] Glasserman, P. (2003) Monte Carlo Methods in Financial Engineering. New York. Springer Science

- [16] Guoping, X. and Zheng, H. (2010) Basket Options valuation for a local volatility jump-diffusion model with the asymptotic expansion method. *Insurance: Mathematics and Economics* **47** 415-422
- [17] Halton, J. (1970) A Retrospective and Prospective Survey of the Monte Carlo Method. *Society for Industrial and Applied Mathematics* **12** 1-63
- [18] Haugh, M. (2005) Martingale Pricing Theory. Financial Engineering: Discrete-Time Asset Pricing. Columbia University.
- [19] Jeroen, V.K. and Stentoft, L. (2010) Multivariate Option Pricing with Time Varying Volatility and Correlations *CREATES Research Paper* **2010-19**
- [20] Knill, O. (2008) Probability and Stochastic Processes with Applications. Harvard University.
- [21] Krekel, M., de Kock, J., Korn, R. and Man, T. (2004) An Analysis of Pricing Methods for Basket Options. *Wilmott Magazine* **3** 82-89
- [22] Luenberger, D.G. (1998) Investment Science. Stanford University. Oxford University Press
- [23] Mazzola, E. and Muliere, P. (2011) Reviewing alternative characterizations of Meixner process. *Probability Surveys* **8** 127-154
- [24] Niederreiter, H. (1992) Random Number Generation and Quasi-Monte Carlo Methods. *Society for industrial applied mathematics*. Philadelphia. Siam
- [25] Owen, A.B. (1997) Scrambled net variance for integrals of smooth functions. *Annals of Statistics* **25** 1541-1562
- [26] Shoutens, W. and Teugels, J.L. (1998) Lévy processes, polynomials and martingales. *Commun. Statist.- Stochastic Models* **14** 335-349.
- [27] Shoutens, W. (2003) Lévy Processes in Finance. West Sussex. John Wiley & Sons Ltd.
- [28] Sköld, M. (2005) Computer Intensive Statistical methods. Lund University. Lund
- [29] Tuffin, B. (1998) Variance Reduction Order using Good Lattice Points in Monte Carlo Methods *Computing* **61** 371-378
- [30] Tuffin, B. (2004) Randomization of Quasi-Monte Carlo Methods for error estimation: Survey and Normal approximation. *Monte Carlo Methods and Applications* **10** 617-628
- [31] Zhang, P.G. (1995) An introduction to exotic options. *European Financial Management* **1** 87-95

- [32] Ökten, G. and Eastman, W. (2004) Randomized quasi-Monte Carlo methods in pricing securities. *Journal of Economic Dynamics and Control* **28** 2399-2426



## A Appendix A

### S&P-500 call option prices

We collected 95 call option prices written on S&P-500 index at the close of market on January 20, 2016 from Nasdaq. The closed index price were  $S_0 = 1881.30$ . We set the risk-free interest rate to 0.03 and the dividend yield to 0. The prices in the table are the calculated mean of bid and ask prices and were used as calibration.

| Strike | April 15<br>2016 | June 17<br>2016 | Sep 16<br>2016 | Dec 16<br>2016 | Jan 20<br>2017 | June 16<br>2017 |
|--------|------------------|-----------------|----------------|----------------|----------------|-----------------|
| 1700   | 179.25           | 195.20          | 212.45         | 226.50         | 232.25         | 250.20          |
| 1750   | 141.30           | 158.95          | 177.95         | 193.15         | 199.20         | 218.55          |
| 1800   | 106.35           | 125.50          | 145.70         | 162.05         | 168.55         | 188.75          |
| 1850   | 75.50            | 95.05           | 116.20         | 133.50         | 139.65         | 160.80          |
| 1900   | 49.25            | 68.50           | 89.95          | 107.10         | 113.25         | 134.85          |
| 1925   | 38.80            | 56.75           | 77.80          | 94.90          | 101.30         | 123.15          |
| 1950   | 29.20            | 46.10           | 66.55          | 83.40          | 89.40          | 111.60          |
| 1975   | 21.30            | 36.70           | 56.20          | 72.70          | 78.75          | 100.65          |
| 2000   | 14.80            | 28.50           | 46.75          | 62.75          | 68.45          | 90.10           |
| 2025   | 9.45             | 21.40           | 38.15          | 52.75          | 58.30          | 79.80           |
| 2050   | 6.25             | 15.95           | 30.80          | 44.85          | 50.85          | 71.05           |
| 2075   | 3.75             | 11.40           | 24.30          | 36.95          | 41.90          | 62.10           |
| 2100   | 2.30             | 8.20            | 18.95          | 30.55          | 35.55          | 54.50           |
| 2150   |                  | 3.70            | 10.60          | 19.40          | 23.15          | 40.15           |
| 2200   |                  | 1.63            | 5.75           | 11.90          | 14.95          | 28.95           |
| 2250   |                  |                 | 2.93           | 6.85           | 8.75           | 19.95           |
| 2300   |                  |                 |                | 3.95           | 5.05           | 13.15           |

Master's Theses in Mathematical Sciences 2016:E32

ISSN 1404-6342

LUTFMS-3303-2016

Mathematical Statistics

Centre for Mathematical Sciences

Lund University

Box 118, SE-221 00 Lund, Sweden

<http://www.maths.lth.se/>